International Journal of Bifurcation and Chaos, Vol. 19, No. 10 (2009) 3347–3371

ON THE WAVELET TRANSFORM APPLICATION TO A STUDY OF CHAOTIC VIBRATIONS OF THE INFINITE LENGTH FLEXIBLE PANELS DRIVEN LONGITUDINALLY

J. AWREJCEWICZ
Technical University of Lodz,
Department of Automatics and Biomechanics,
Stefanowskiego Str. 1/15, 90-924 Lodz, Poland
awrejcew@p.lodz.pl

A. V. KRYSKO* and V. SOLDATOV
Saratov State Technical University,
Department of Higher Mathematics,
410054 Saratov, Russia
**tak@san.ru*

Received December 18, 2008; Revised February 4, 2009

Both classical Fourier analysis and continuous wavelets transformation are applied to study nonlinear vibrations of infinitely long flexible panels subject to longitudinal sign-changeable external load actions. First the governing PDEs are derived and then the Bubnov–Galerkin method is applied to yield 2N first order ODEs. The further used Lyapunov exponent computation is described. Transition scenarios from regular to chaotic dynamics of the being investigated plate strip are analyzed using different wavelets, and their suitability and advantages/disadvantages to nonlinear dynamics monitoring and quantifying are illustrated and discussed. A few novel results devoted to the beam nonlinear dynamics behavior are reported. In addition, links between the largest Lyapunov exponent computation and the wavelet spectrum numerical estimation are also illustrated and discussed.

Keywords: Wavelets; plate strip; stability; chaos.

1. Introduction

Wavelet analysis has been introduced by Grossman and Morlet in the early 1980s [Grossman & Morlet, 1984]. Nowadays there exists a considerable number of references associated with wavelet analysis, and hence we point out only some of them [Daubechies, 1991; Daubechies & Bates, 1993; Newland, 1993; Chui, 1997; Astafieva, 1996].

It is already well recognized that the mechanical object characteristics based on power spectra analysis in the frame of Fourier transform yielding the signal representation only in frequency domain are not complete. Therefore, in this work, the frequency-temporal characteristics are reported with a use of the continuous wavelet-transformation. This wavelet-based novel field of analysis finds applications in signal processing and signal synthesis (for instance, in language recognition), in the analysis of transformations of various type, in the investigation of the turbulent field properties, in finding solutions to equations [Lepik, 2001, 2007], in pattern recognition in human

vision, image compression, radar and earthquake prediction, de-noising of noising data as well as in economical packing of large amount of information.

In mechanical civil engineering, the majority of research oriented on wavelets application concerns identification, localization and damage detections.

Fedorova and Zeitlin [1998] studied dynamics of storage rings, optimal dynamics of mechatronic systems, and beam vibration governed by PDEs. The wavelet-oriented construction was proposed to find solutions to the obtained PDEs.

Staszewski [1998] used the continuous Grossman–Morlet wavelets to identify nonlinear systems applying the slowly-varying, time-dependant amplitude and phase functions in order to detect frequency localization in a multi-degree-of-freedom system. Then, Staszewski and his coworkers, applied wavelet transform for damage detection via optical measurements [Patsias & Staszewski, 2002] as well as for structural health monitoring [Staszewski & Robertson, 2007]. A two-dimensional wavelet transform was used for identification of cracks in plate structures in [Loutridis, 2005].

It should be mentioned that the wavelet analysis devoted to rigid body investigations is still rather rarely applied [Ghanem & Romeo, 2001; Jeong, 2001; Lepik, 2001].

Liu [2003] applied an adaptive wavelet transform using the flexibility of the generalized harmonic wavelets to study simulated and vibration signals.

Practical example of diagnosis for rotating machinery using both neural networks and wavelet transforms was presented by Sanz *et al.* [2007]. The applied method allowed to detect the novelties and anomalies of faulty signals of the experimental vibration data of a gearbox.

In [Permann & Hamilton, 2007] the classical Duffing oscillator was investigated using the Daubechies wavelets, whereas in [Zheng *et al.*, 1998] the Newland wavelets were applied to study vibrations of a rotor. Wong and Chen [2001] applied the Morlet wavelets for the case, when a frequency of periodic vibrations changes in time.

In [Nouira *et al.*, 2008] experimental study of the beam-damp interface is carried out, and the wavelet transform has been applied to monitor the instantaneous frequencies and damping. It allowed the authors to determine the spatial distribution of microsliding and tangential force along the contact interface. Zhong and Oyadiji [2008] proposed an approach based on auxiliary mass spatial probing by stationary wavelet transform (SWT) to detect cracks in beam-like structure. Natural frequencies curve was decomposed by SWT into approximation coefficient useful for damage detection. Sixty-four cases have been studied using SWT and FEM. The effects of crack depth, crack location, auxiliary mass and advantages of the applied method was also been verified via an experimental test. In the paper [Ji & Chang, 2008] a nontarget stereo vision technique to measure the response of a line-like structure simultaneously in both spatial and temporal domains is developed. After reconstruction of a spatio-temporal displacement, wavelet transform is applied to get the modal characteristics. The applied method has been illustrated using a steel cantilever beam and a bridge stay cable.

Yang *et al.* [2008] studied a double-cracked beam and a plate with multiple cracks using the discrete wavelet transform. Numerical and experimental results were compared showing a good agreement.

Bayissa *et al.* [2008] presented a novel damage identification technique based on the statistical moments of the energy density function of the vibration response in time and frequency domains. The wavelet coefficients are transformed into a new damage identification parameter in the space domain. The refinements of damage detection on transversally vibrating structural components aiming at significant reduction of the border distortions normally arising during wavelet procedure were proposed by Messina [2008]. The effectiveness of the applied algorithm is demonstrated via numerical and experimental examples.

Blasting vibration signal was studied using wavelets in [Zhong *et al.*, 2008]. The wavelet frequency band energy was studied and intensity, frequency and vibration duration have been monitored.

An application of the wavelet transform to damage detection of a beam-spring structure was illustrated in [Zhu *et al.*, 2008].

A new technique for detection and diagnosis of rolling bearing faults was proposed and illustrated by Al-Raheem *et al.* [2008]. The results for both real and simulated bearing vibration data show the effectiveness of the proposed approach. Li *et al.* [2008] developed the wavelet transform-based higher-order statistics for fault diagnosis in rolling element bearings. The results demonstrated show

high applicability of the proposed method in vibration signal processing and fault diagnosis.

In the case of archetype models for chaotic oscillations often the Duffing, Van der Pol and Lorenz equations are analyzed [Moslehy & Evan-Iwanovski, 1991; Konishi, 2001; Ghanem & Romeo, 2001; Ribeiro, 2001; Xiaoping, 2001]. As it will be shown further our research is also associated with the classical archetype model of chaos, i.e. with the Duffing oscillator. It should be emphasized that there are two references closely related to our research, i.e. [Moshlehy & Evan-Iwanovski, 1991; Konishi, 2001]. It has been shown in [Moslehy & Evan-Iwanovski, 1991], how the change of parameters of the Duffing equation may yield its chaotic oscillations, whereas in [Konishi, 2001] the external force is used as the control parameter, to study regular and chaotic dynamics. Lepik [2003] applied a discrete-wavelet transformation and the wavelet-like algorithms packets to study the Duffing equation. In [Awrejcewicz & Krysko, 2003b] a state of art review and application of wavelet analysis to flexible continuous systems was proposed. On contrary to the considered aspects, we mainly aim on the application of continuous wavelet-transformation allowed for carrying out simultaneously analysis in both time and frequency domains.

In what follows we study nonlinear vibrations of infinitely long flexible panels subjected to longitudinal sign-changeable external load actions. In order to study complex dynamics of the mentioned objects and in particular transitions from regular to chaotic vibrations two fundamental methods are applied: the frequency-time analysis on the basis of continuous wavelet transformation and dynamics monitoring of the Lyapunov exponents. In addition, the classical Fourier analysis is also applied. Since there exists many different wavelets used to study engineering objects, one of our paper targets is to answer an important question: Which of these used in literature wavelets are most suitable to study nonlinear vibrations of mechanical systems?

2. Statement of the Problem

Let us consider nonlinear vibrations of infinitely long plate strip subjected to action from a longitudinal sign-changeable load assuming that one of the plate dimensions differs essentially from a second one: $a \ll b$ (Fig. 1).

The possible boundary layer effects are neglected during our study. It is assumed that the

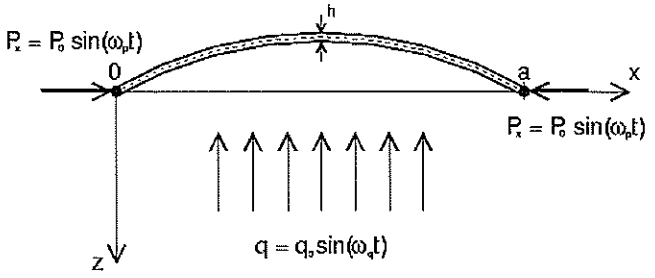

Fig. 1. The investigated system.

plate strip is cylindrically deformed along its length. Therefore, it is sufficient to study the beam strip of length a, and unit wideness, i.e. we study a 1D problem with one space coordinate. Equation of motion reads [Volmir, 1972]:

$$\frac{h\gamma}{g}\ddot{w} + h\varepsilon\dot{w} = -D\frac{\partial^4 w}{\partial x^4} + \frac{Eh}{2a(1-\nu^2)} \times \left\{\int_0^a \left(\frac{\partial w}{\partial x}\right)^2 dx\right\}\frac{\partial^2 w}{\partial x^2} - P_x(t)\frac{\partial^2 w}{\partial x^2}, \tag{1}$$

where $w(x,t)$ is the beam-strip deflection, x is the space coordinate, t denotes time, a is the beam-strip length, h denotes its thickness, ν is the Poisson coefficient, $P_x(t)$ is the longitudinal load, $D = (Eh^3/12(1-\nu^2))$ is the plate-strip cylindrical stiffness, γ is the plate-strip weight density, g is the Earth acceleration, and ε denotes damping coefficient.

We are going to reduce the governing equation to its nondimensional form by introducing the nondimensional quantities denoted with bars:

$$x = a\bar{x}, \quad w = h\bar{w}, \quad P_x(t) = \frac{Eh^3}{a^2}\bar{P}_x(t),$$
$$q = \frac{Eh^4}{a^4}\bar{q}(x,t), \quad t = \frac{a^2}{h}\sqrt{\frac{\gamma}{Eg}}\bar{t}, \tag{2}$$
$$\varepsilon = \frac{a^2}{h}\sqrt{\frac{\gamma}{Eg}}\bar{\varepsilon}, \quad \lambda = \frac{1}{12(1-\nu^2)}.$$

As a result Eq. (1) is cast to the form:

$$\ddot{w} + \varepsilon\dot{w} = -\lambda\frac{\partial^4 w}{\partial x^4} + 6\lambda\left\{\int_0^a \left(\frac{\partial w}{\partial x}\right)^2 dx\right\}\frac{\partial^2 w}{\partial x^2} - P_x(t)\frac{\partial^2 w}{\partial x^2} \tag{3}$$

In derived Eq. (3) bars are already omitted. The boundary condition of a simple support has

the form

$$w = w_x'' = 0 \quad \text{for } x = 0, 1 \tag{4}$$

and the following initial conditions are applied

$$\begin{aligned} w(x)|_{t=0} &= w_0 \sin(\pi x), \\ \dot{w}(x)|_{t=0} &= 0. \end{aligned} \tag{5}$$

Further steps of mathematical modeling follow references [Awrejcewicz *et al.*, 2002; Awrejcewicz & Krysko, 2003a; Awrejcewicz *et al.*, 2007].

In order to reduce the initial-boundary value problem to a system of ODEs, we apply the Bubnov–Galerkin approach. A solution is sought in the following form

$$w(x,t) = \sum_{i=0}^{N} A_i(t) w_i(x), \tag{6}$$

where $w_i(x)$ should satisfy the boundary conditions of the stated problem. The following system of ODEs is finally obtained regarding amplitudes $A_i(t)$:

$$\begin{aligned} &\sum_{i=0}^{N} (\ddot{A}_i + \varepsilon \dot{A}_i) a_{ik} \\ &\quad = -\lambda \sum_{i=0}^{N} A_i b_{ik} + 6\lambda L(\{A_i\}_1^N) \\ &\qquad \times \sum_{i=0}^{N} A_i c_{ik} - P_x(t) \sum_{i=0}^{N} A_i c_{ik}, \end{aligned} \tag{7}$$

where $k = 0, 1, \ldots$ and

$$\begin{aligned} a_{ik} &= \int_0^1 w_i(x) w_k(x) dx, \\ b_{ik} &= \int_0^1 w_i^{IV}(x) w_k(x) dx, \\ c_{ik} &= \int_0^1 w_i''(x) w_k(x) dx, \\ L(\{A_i\}_1^N) &= \int_0^1 \left\{ \sum_{i=0}^{N} A_i(t) w_i'(x) \right\}^2 dx. \end{aligned} \tag{8}$$

The system of the obtained second order ODEs is then transformed to a system of first order ODEs that are solved via one of the Runge–Kutta methods. Let us consider the solution to Eq. (3) with simply supported boundary conditions of the form (4) and initial conditions (5). Basis functions associated with the Bubnov–Galerkin method application are taken in the following form: $\{\sin \pi(2i + 1)x\}_{i=0,\ldots,N}$, and they satisfy the boundary conditions. Therefore, the following form of solution is sought:

$$w(x,t) = \sum_{i=0}^{N} A_i(t) \sin(\pi(2i+1)x). \tag{9}$$

Substitution of (9) into (3) yields

$$\begin{aligned} \sum_{i=0}^{N} (\ddot{A}_i + \varepsilon \dot{A}_i) \sin(\pi(2i+1)x) &= -\lambda \sum_{i=0}^{N} A_i (\pi(2i+1))^4 \sin(\pi(2i+1)x) \\ &\quad + \{6\lambda L(\{A_i\}_1^N)\} - P_x(t) \sum_{i=0}^{N} A_i (\pi(2i+1))^2 \sin(\pi(2i+1)x), \end{aligned}$$

$$\begin{aligned} L(\{A_i\}_1^N) &= \int_0^1 \left\{ \sum_{i=1}^{N} A_i (\pi(2i+1)) \cos(\pi(2i+1)x) \right\}^2 dx \\ &= \sum_{i=1}^{N} \sum_{j=1}^{N} \int_0^1 A_i A_j (\pi^2 (2i+1)(2j+1)) \cos(\pi(2i+1)x) \\ &\quad \times \cos(\pi(2j+1)x) dx \\ &= \sum_{i=1}^{N} \int_0^1 \{A_i (\pi(2i+1)) \cos(\pi(2i+1)x)\}^2 dx \\ &= \frac{\pi^2}{2} \sum_{i=1}^{N} \{A_i (\pi(2i+1))\}^2. \end{aligned} \tag{10}$$

Multiplication of both sides of Eq. (10) by $\sin(\pi(2j+1)x)$ and integration regarding x from 0 to 1 gives:

$$\sum_{i=0}^{N}(\ddot{A}_i + \varepsilon\dot{A}_i)\int_0^1 \sin(\pi(2i+1)x) \times \sin(\pi(2j+1)x)dx = -\lambda\sum_{i=0}^{N} A_i(\pi i)^4 \int_0^1 \sin(\pi(2i+1)x) \times \sin(\pi(2j+1)x)dx + \{6\lambda L(\{A_i\}_1^N)\} - P_x(t)\sum_{i=0}^{N} A_i(\pi i)^2 \int_0^1 \sin(\pi ix)\sin(\pi jx)dx. \tag{11}$$

Note that the functions $\{\sin(\pi ix)\}_1^N$ are mutually orthogonal in the interval of $[0;1]$, and finally the following equations are obtained:

$$\ddot{A}_j + \varepsilon\dot{A}_j = -\lambda A_j(\pi j)^4 + \left(3\lambda\pi^2\sum_{i=0}^{N}(A_i i)^2 - P_x(t)\right)A_j(\pi j)^2, \quad j = 1, 2, \ldots, N. \tag{12}$$

Therefore, N ordinary differential equations of the second order are obtained. Substitution of $A'_j(t) = \dot{A}_j(t)$ allows to reduce the problem to that of $2N$ first order ODEs of the form:

$$\begin{cases} \dot{A}_j = \dot{A}'_j; \\ \dot{A}'_j = -\varepsilon A'_j - \lambda A_j(\pi j)^4 + \left(3\lambda\pi^2\sum_{i=0}^{N}(A_i i)^2 - P_x(t)\right)A_j(\pi j)^2, \end{cases} \tag{13}$$

which are then solved by one of the Runge–Kutta methods. It is clear that for a lack of initial deflection the solution is equal to zero. Therefore the initial conditions are taken in the form of (5), where w_0 serves as a small initial deflection. Owing to the structure of Eq. (13) one may observe that an initial perturbation of a first harmonic is not propagated into higher order harmonics, and hence the coefficients standing by higher harmonics are equal to zero. Therefore, in this case the system of Eqs. (11) is cast to the form of the following second order equation:

$$\ddot{A}_1 + \varepsilon\dot{A}_1 = -(\lambda\pi^2(1+3A_1^2) - P_x(t))A_1\pi^2. \tag{14}$$

Observe that the obtained equation is the well-known Duffing equation [Nayfeh & Mook, 1979]. In what follows we apply only excitation in the form of $P_x = p_x\sin\omega t$.

The approximated analytical periodic solutions to the Duffing equation can be found using perturbation techniques widely described in the works of Guckenheimer [1983], Holmes and White [1983], Nayfeh and Balachandran [1995]. It should be emphasized that solutions obtained via perturbation techniques yield reasonable approximation only in the case of small loading and small damping. For instance, Holmes [1979] has shown that in the case of moderate loading values and presence of damping, the approximated analytical approaches may yield doubtful results.

In order to apply a numerical procedure we reduce Eqs. (14) to a system of first order differential equations. Introduction of notation $y_1 = A_1$, $y_2 = y'_1$ yields the following, equivalent to Eq. (14), form

$$\begin{aligned} y'_1 &= y_2, \\ y'_2 &= -\varepsilon\dot{A}_1 - (\lambda\pi^2(1+3A_1^2) \\ &\quad - p_x\sin\omega t)A_1\pi^2. \end{aligned} \tag{15}$$

In what follows we are focused on a study of regular and chaotic dynamics of the Duffing equation with the use of the Lyapunov spectrum investigation.

3. The Lyapunov Exponents

The Lyapunov exponents play an important role in the theory of Hamiltonian and dissipative systems. They allow measurement of a noisy level of a nonlinear system. Besides, there is a link between the Lyapunov exponents and other characteristic features of chaotic dynamics, like a Kolmogorov entropy and a fractal dimension. The Lyapunov exponents characterize an averaged speed of the neighborhood trajectories' divergence.

Let us assume that after application of one of the methods yielding reduction of an infinite problem to finite one, the following set of first order nonlinear ODEs is obtained (in our case this is represented by system (15))

$$\frac{dY}{dt} = F(x,t). \tag{16}$$

In this paper, we follow the algorithm of Lyapunov exponents computation developed by Benettin *et al.* [1976, 1979, 1980].

Let us consider two neighborhood trajectories with the initial conditions Y_0 and $Y_0 + \Delta Y_0$. Its time evolution yields tangent vector $\Delta Y(Y_0, t)$ of the length

$$d(Y_0, t) = \Delta Y(Y_0, t). \tag{17}$$

Dynamics ΔY is governed by linearization of Eq. (16):

$$\frac{\Delta Y}{dt} = \frac{\partial \mathbf{F}}{\partial Y} \cdot \Delta Y, \tag{18}$$

where $\partial \mathbf{F}/\partial Y$ is the Jacobi matrix for $\mathbf{F}(Y, \mathbf{M})$. Let us define an averaged speed of exponential divergence of the neighborhood trajectories

$$\lambda(Y_0, \Delta Y_0) = \lim_{\substack{t\to\infty \\ d(0)\to 0}} \frac{1}{t} \ln \frac{d(Y_0, t)}{d(Y_0, 0)}. \tag{19}$$

One may prove that a convergence interval of λ exists and is bounded. In addition, there exists a full system of m fundamental solutions $(\mathbf{e}_i)$ of Eq. (18), and each of them is characterized by velocity λ of the following defined value:

$$\lambda_i(Y_0) = \lambda(Y_0, e_i), \tag{20}$$

which are the well known Lyapunov characteristic exponents. They do not depend on a metric of a space phase [G], and they can be ordered as follows:

$$\lambda_1 \geq \lambda_2 \geq \lambda_3 \geq \cdots \geq \lambda_M.$$

In a particular case of a periodic trajectory, Eq. (18) can be interpreted as a mapping on a period T, which can be given in the form

$$\Delta Y_{n+1} = \mathbf{A} \cdot \Delta Y_n. \tag{21}$$

Matrix $\mathbf{A}$ possesses M eigenvalues α_M having (in general) a complex form:

$$|\alpha_1| \geq |\alpha_2| \geq \cdots \geq |\alpha_M|. \tag{22}$$

Let us denote the corresponding eigenvectors by $\mathbf{e}_i$. Then (18) for $\Delta Y_0 = \mathbf{e}_i$ yields

$$\Delta Y_n = \alpha_i^n \mathbf{e}_i. \tag{23}$$

Then owing to (19) one gets

$$\lambda_i(\mathbf{e}_i) = \frac{1}{T} \ln |\alpha_i| = \lambda_i.$$

On the other hand, one may conclude from (23) that for

$$\Delta Y_0 = c_1 \mathbf{e}_1 + \cdots + c_M \mathbf{e}_M = \sum_{i=1}^{M} c_i \mathbf{e}_i$$

the dynamics of the vector ΔY_n is governed by a first nonvanishing coefficient c_i. Observe that each of the Lyapunov exponents defines velocity λ in a certain subspace having dimension smaller on unit amount than a previous one. It means that almost for all ΔY we have $\lambda = \lambda_1$.

A generalization of eigenvalues and eigenvector notions has been extended to periodic orbits by Oseledec [1968]. This idea is mainly based on observation that also nonperiodic orbits can be approximated by periodic ones but with sufficiently long periods.

For any continuous trajectory governed by differential equations (15), at least one of the Lyapunov exponents associated with a vector tangent to a trajectory must be equal to zero.

The Lyapunov exponents for vectors ΔY are also called first order exponents. Oseledec [1968] generalized that notion for an averaged velocity of exponential growth of p-dimensional volume V_p built on the vectors $\Delta Y_1, \Delta Y_2, \ldots, \Delta Y_n$, $(p \leq M)$. It is clear that

$$\lambda^p(Y_0, V_p) = \lim_{t\to\infty} \frac{1}{t} \ln \frac{V_p(Y_0, t)}{V_p(Y_0, 0)} \tag{24}$$

is exactly a Lyapunov exponent of p order. Oseledec [1968] as well as Benettin *et al.* [1976] have shown that $\lambda^p(Y_0, V_p)$ are defined via a first order sum p. Proceeding in an analogous way for almost all ΔY the following relation holds $\lambda(Y_0, \Delta Y) = \lambda_1(Y_0)$, as well as for almost all V_p we have

$$\lambda^p = \lambda_1 + \lambda_2 + \cdots + \lambda_p = \sum_{i=1}^{p} \lambda_i. \tag{25}$$

Relation (25) is used for numerical approximation of the Lyapunov exponents. For $p = M$ one gets an averaged velocity of exponential growth of the phase volume:

$$\lambda^M = \sum_{i=1}^{M} \lambda_i(Y_0). \tag{26}$$

Maximal exponent λ_1 is often used as chaos criterion. Recall that $\lambda(Y_0, \Delta Y_0) = \lambda_1(Y)$ for almost all tangent vectors ΔY_0. Therefore, for λ_1 computation an initial vector ΔY_0 can be taken arbitrarily. Integrating Eqs. (15) and (18) simultaneously one finds $d(t) = |\Delta Y(t)|$, and further for convenience $d_0 = d(0) = 1$ is taken. Problems occur when $|\Delta Y|$ increases exponentially, since computational errors appear. Application of the linearized equation has one important advantage. Namely, its solution does not depend on $|\Delta Y|$. However, in some cases integration of both trajectories is required.

Let us take time interval τ and let us rescale $|\Delta Y|$ into one at the end of each interval, i.e. we preserve the vector length $|\Delta Y|(|\Delta Y|) \to d_0 = 1$, without change of its direction. Let us introduce the notion of $\tilde{Y} = Y + \Delta Y$, and let τ be a finite time interval. Therefore, we successively compute

$$d_k = |\Delta Y_{\mathbf{k-1}}(\tau)|, \tag{27}$$

$$\Delta Y_k(0) = \frac{\Delta Y_{k-1}(\tau)}{d_k}, \tag{28}$$

where $\Delta Y_{\mathbf{k-1}}(\tau)$ are obtained via integration of (16), (19) on interval τ with initial values $Y(k\tau)$, $\Delta Y_k(0)$. Assuming

$$\lambda_n = \frac{1}{n\tau}\sum_{i=1}^{n} d_i, \tag{29}$$

(19) yields

$$\lambda_1 = \lim_{n\to\infty} \lambda_n. \tag{30}$$

For regular dynamics $\lambda_1 = 0$, whereas for chaotic one we have $\lambda_1 > 0$, which does not depend on Y. The so-far described method is applicable either for phase flow or for cascades (maps).

4. The Benettin *et al.* Algorithm

The proposed algorithm by Benettin *et al.* [1976] allows for computation of full spectrum of Lyapunov exponents in M-dimensional phase space.

Let us take an initial basis from p orthonormalized tangent vectors and let us numerically define a p-dimensional volume $V_p(t)$ defined by those vectors. It allows finding the Lyapunov exponent λ_1^p of order p (24). Applying so-far presented procedure for $p = 1, 2, \ldots, M$, one gets from (25) all exponents $\lambda_1, \lambda_2, \ldots, \lambda_M$. Since during movements the angles between tangent vectors exponentially decrease, numerical errors increase. Therefore, lengths of vectors ΔY should be also periodically orthogonalized. In addition, new created vectors should occupy the same space as the old (being orthogonalized) ones. Here, the so-called Gramm–Schmidt renormalization procedure can be applied. Let $\Delta Y_{k-1}(\tau)$ be a tangent vector in time instant at the beginning $\Delta Y_{k-1}(0)$. First, we compute for each time interval τ the following quantities

$$d_k^{(1)} = |\Delta Y_{k-1}^{(1)}(\tau)|, \tag{31}$$

$$\Delta Y_{\mathbf{k}}^{(1)} = \frac{\Delta Y_{\mathbf{k-1}}^{(1)}}{d_k^{(1)}}. \tag{32}$$

Now, for $j = 2, \ldots, M$ the following quantities are successively defined

$$\mathbf{u}_{\mathbf{k-1}}^{(i)}(\tau) = \Delta Y_{\mathbf{k-1}}^{(j)}(\tau) - \sum_{i=1}^{d-1}(\Delta Y_{\mathbf{k}}^{(i)}(0) \cdot \Delta Y_{\mathbf{k-1}}^{(j)}(\tau) \cdot \Delta Y_{\mathbf{k}}^{(i)}(0)), \tag{33}$$

$$d_k^{(j)} = |\mathbf{u}_{k-1}^{(j)}(\tau)|, \tag{34}$$

$$\Delta Y_k^{(j)}(0) = \frac{\mathbf{u}_{k-1}^{(j)}(\tau)}{d_k^{(j)}}. \tag{35}$$

In what follows, in the duration of $(k-1)$-th interval of time τ, the volume V_p increases by $d_k^{(1)}$ $d_k^{(2)}$ $\cdots$ $d_k^{(p)}$ times.

Therefore, (30) gives

$$\lambda_1 = \lim_{n\to\infty} \frac{1}{n\tau} \ln(d_i^{(1)} \quad d_i^{(2)} \quad \cdots \quad d_i^{(p)}). \tag{36}$$

Computation of $\lambda_1^{(p-1)}$ from $\lambda_1^{(p)}$, and application of formula (25) allow finding the pth Lyapunov exponent

$$\lambda_p = \lim_{n\to\infty} \frac{1}{n\tau}\sum_{i=1}^{n} \ln d_i^{(p)}. \tag{37}$$

5. Transitional Regimes

In general the Lyapunov exponents are used to quantitatively describe either periodic or chaotic orbits. Theoretical results reported in the above are further used in our paper for chaos criteria. However, in real systems (in particular, in continuous mechanical systems) often, another behavior takes place. Namely, transition from chaotic to regular dynamics and vice versa occurs. Widely applied classical methods devoted to the investigation of dynamical systems deal with the construction of a phase space and its various projections (phase portraits), construction of the frequency spectra with the help of FFT, and also the Poincaré maps. Observe that the latter ones do not allow to follow time histories of the system frequencies, and recently to get more information from the analyzed system a wavelet transformation is applied.

6. Wavelet Transformation versus Nonstationary Signals

Investigation of signals representing data using function superposition goes back to Joseph Fourier (early 1800's), when he applied only sines and

cosines to estimate various functions. It is well known that one of the fundamental characteristics of the studied quasi-periodic and chaotic dynamics is frequency spectrum of the vibration process. The characteristics mentioned define dispersion distribution (averaged squared value) of the frequencies. Typically, in order to estimate a density of the power spectra the Fast Fourier Transform (FFT) with successive averaged spectrum histories is applied. Note that the application of the integral transformation and the Fourier series is very useful and illustrative since all transformations are carried out with the help of two real functions: $\sin(t)$, $\cos(t)$ or equivalently one complex wave $\exp(it) = \cos(t) + i\sin(t)$, $i = \sqrt{-1}$, and are easily proved.

On the contrary, during wavelet analysis the scale used to study various data plays a key role. Namely, we can use large and small "windows" by applying two main wavelet-tool properties, i.e. different *scales* and *resolutions*. The wavelet transform was introduced recently and its mathematical description is still under development. As it has been already mentioned, the term "wavelet", denoting a small wave, was first introduced by Grossman and Morlet [1984] in the middle 80's. Nowadays, various wavelet-type analyzers are widely applied in various branches of science but not on nonlinear dynamics of beams, plates and shells. The wavelet-transform of a one-dimensional (1D) signal consists of the development into a basis constructed via soliton-like functions called wavelet, using various interval transformations and shifts. Each of the basic functions quantifies the studied signal frequency and its time localization. Therefore, the wavelet-transform represents a 2D signal picture, where frequency and time are considered to be independent quantities. This is why one may study the signal properties simultaneously in time and frequency domains.

The wavelet-type studies are focused on a choice of the so-called *mother wavelet* or an *analyzing wavelet*. One mother (prototype) wavelet allows to perform the detailed frequency (low frequency version) and temporal (high frequency version) analysis of the data being investigated. This is achieved by using coefficients in a linear combination of the wavelet functions. Since a wavelet transformation is a scalar product of the analyzing wavelet and a signal under analysis, the coefficients $W(t,\omega)$ represent a combinational information of both wavelet and signal (the same is held for the Fourier coefficients, which contain information on the signal and the sinusoidal wave). In this work in order to study chaotic vibrations of the Timoshenko beam we apply a few wavelet transforms and show that each of them possesses its own peculiar characteristics in time and frequency domains. Many researchers called the wavelet analysis "mathematical microscope" since the methods keep good resolution on different scales. Parameter t concentrates the "mathematical microscope" focus, the scale coefficient ω allows to magnify the signal, and finally the "optical quality" of the microscope is defined via the choice of the basis wavelet ψ.

Real bases are often constructed using derivatives of the Gauss functions

$$\psi_m(t) = (-1)^m \frac{\partial^m \left[\exp\left(-\frac{|t|^2}{2}\right)\right]}{\partial t^m},$$

$$\widehat{\psi}_m(k) = m(ik)^m \exp\left(-\frac{|k|^2}{2}\right),$$

where $\widehat{\psi}_m(k)$ represent the Fourier transform.

Higher derivatives possess more zero order moments and hence allow to detect some peculiar higher order signal features.

Often a complex basis is constructed in the space of k and t using the so-called Morlet wavelet [Grossman & Morlet, 1984], characterizing a flat wave being modulated by a Gaussian of unit wideness. The mentioned wavelet functions and their Fourier transformations are as follows:

$$\psi_m(t) = \exp(ik_0 t)\exp\left(-\frac{|t|^2}{2}\right),$$

$$\widehat{\psi}_m(k) = H(k)\exp\left(-\frac{(k-k_0)^2}{2}\right),$$

where $H(k)$ is the Heaviside function.

Observe that increase of k_0 improves the angle basis selectivity, whereas its space selectivity decreases.

In Figs. 2(a)–2(c) the Gauss wavelets are shown obtained for $m = 1; 2; 8$ depending on time (upper row) and their Fourier transforms (lower row), as well as the Morlet wavelet for $k_0 = 15$ [Fig. 1(d)].

The wavelet for $m = 1$ is named WAVE-wavelet, whereas for $m = 2$ it is called the MHAT-wavelet or the Mexican hat. The Gauss wavelet for $m = 2$ has narrow energetic spectrum and two zero moments, whereas for $m = 8$, it has six zero moments and is well adapted for complex signals analysis. The so-far presented wavelets are further used in our paper.

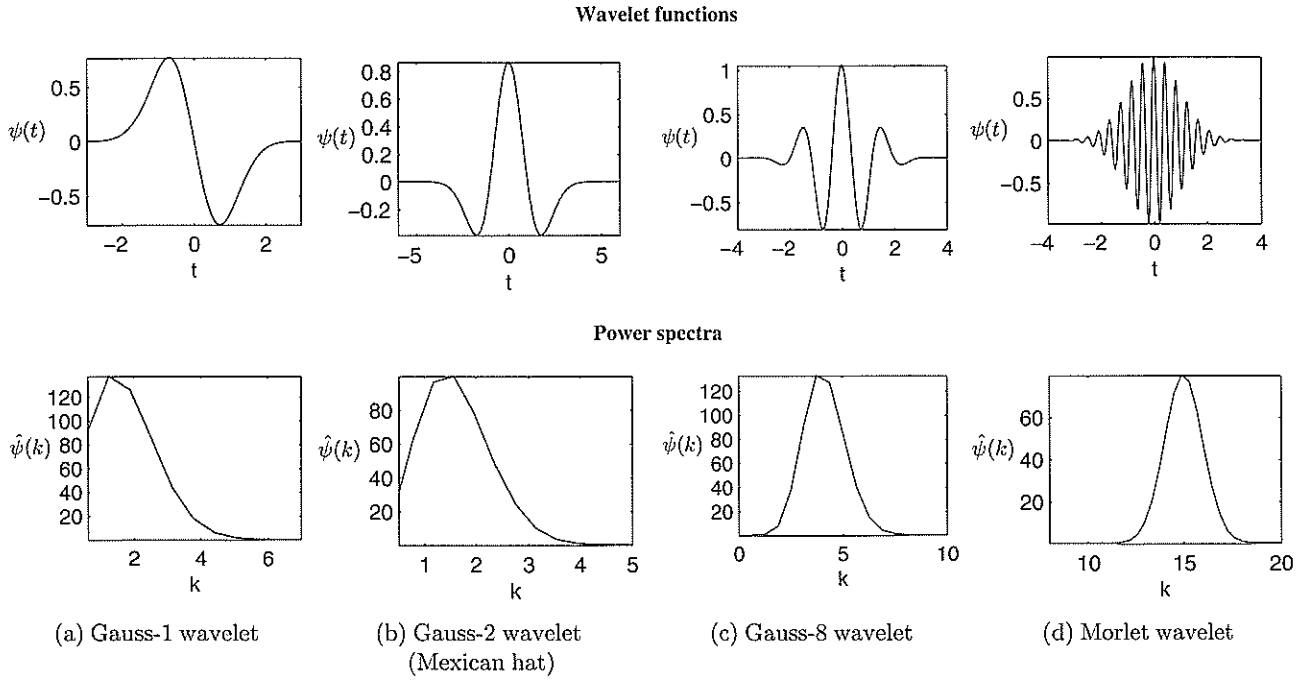

(a) Gauss-1 wavelet (b) Gauss-2 wavelet (Mexican hat) (c) Gauss-8 wavelet (d) Morlet wavelet

Fig. 2. Wavelet functions and the corresponding power spectra.

In tables, the wavelet spectra of a 1D signal, i.e. $|W(t,\omega)|$ are shown as surfaces in 2D and 3D spaces as well as their projections onto the plane (t,ω) in the form of color pictures, power spectra, phase portraits as well as the Lyapunov exponents evolution (in our case, two Lyapunov exponents are monitored).

The color pictures given in the tables allow to trace changes of the wavelet-transform coefficients on various scales and versus time, as well as, graphs of local extremes of the mentioned surfaces (the so-called skeletons) evidently characterizing a structure of a being analyzed process. In tables, we have time on horizontal axes, whereas on vertical axes time scale is shown. Bright (dark) areas correspond to large (small) values of energy density $|W(t,\omega)|$. The sequence of wavelets is the same for all tables: Morlet wavelet, WAVE-wavelet, Mexican hat wavelet, and the Gauss-8 wavelet.

The mathematical model of the mechanical system being studied — Eq. (15) — consists of two control parameters: frequency ω and loading amplitude p_x. Changing those parameters, one may study various vibration regimes. In Table 1, for instance, classical results regarding harmonic vibrations are reported.

The phase portrait and the power spectrum indicate that the oscillations are harmonic. Coming back to wavelets, it is clear that not all of them yield enough clear signal characteristics. Observe that the wideness of Mexican hat and WAVE wavelets are so broadband, that an extraction of the signal frequency is difficult. The most suitable for this purpose is the Morlet wavelet, and then the Gauss-8 wavelet, and the frequency yielded by them fits well to the standard by Fourier spectrum analysis. However, the main wavelet analysis the advantage of in comparison to the Fourier ones is that we may monitor the frequency spectrum changes versus time. In other words, assuming that we have, at hand, estimated well the frequency from the wavelets, one may conclude that Table 1 reports the frequency oscillations to be constant in time.

One may expect on a basis of theoretical background that the Lyapunov exponents in this case are negative (lack of chaos). Besides, increase of computational time yields their asymptotic limiting values.

In Table 2, principally different behavior is obtained. The largest Lyapunov exponent is positive, and matching this observation with the broadband Fourier spectrum and the phase portrait allows to conclude the chaos occurrence. The wavelet spectra are in favor of that conclusion.

The chaos identification elements like a phase portrait and a Fourier spectrum yield the integral information on the system within the monitoring time interval. Even for unchanged values of the

Table 1. $(\omega = 2; p_x = 3)$.

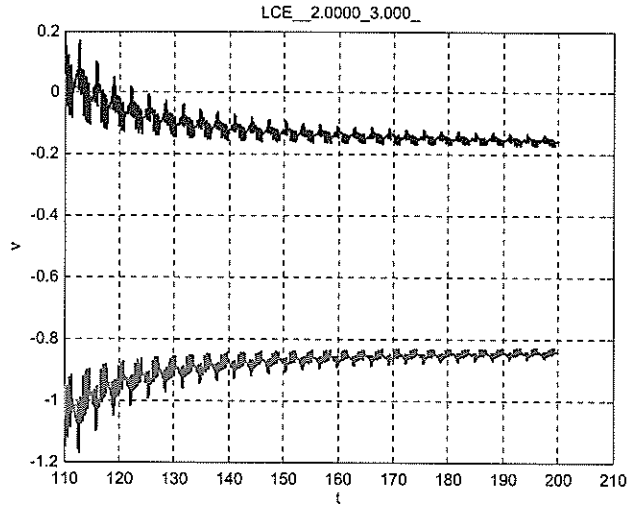

The Lyapunov exponents

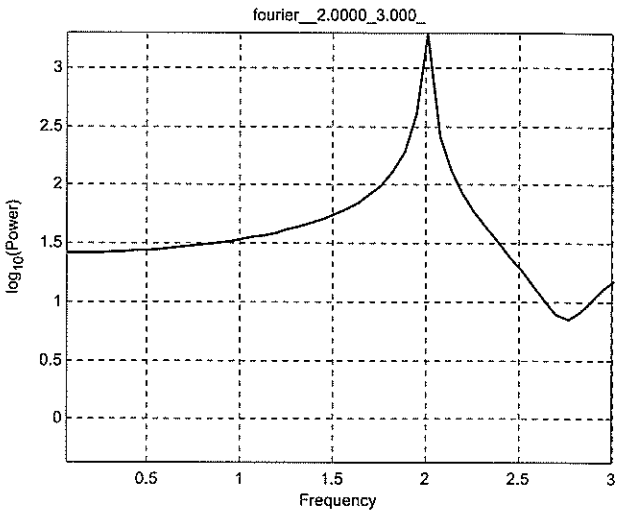

Power spectrum

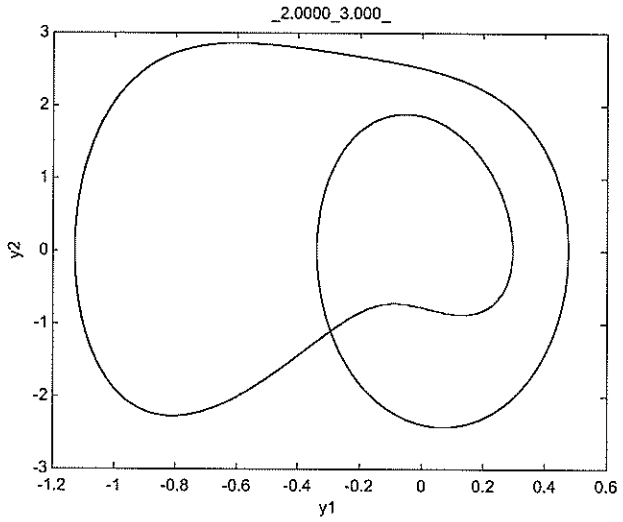

Phase portrait

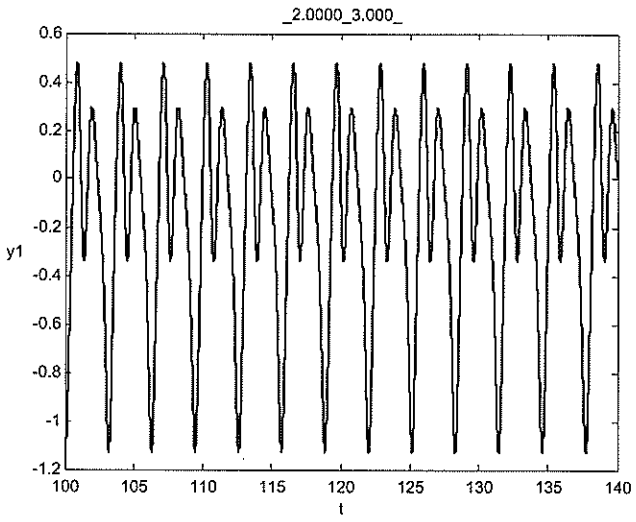

Time history

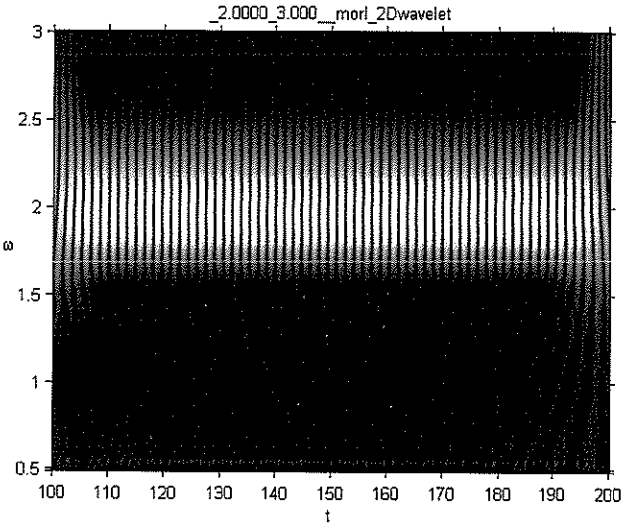

The Morlet wavelet

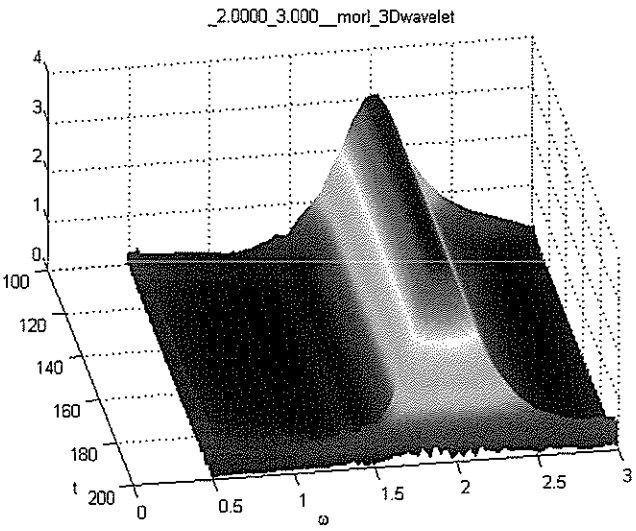

The Morlet wavelet

Table 1. (*Continued*)

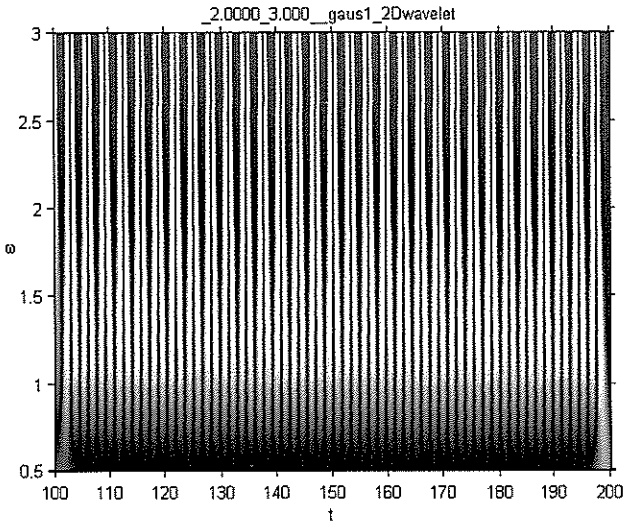

The Gauss-1 wavelet

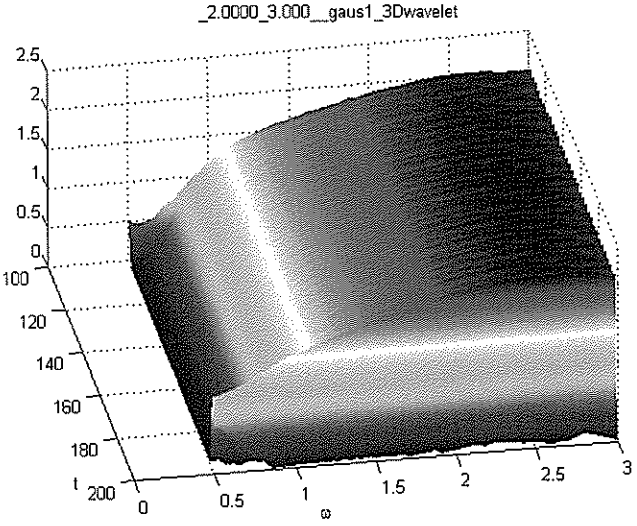

The Gauss-1 wavelet

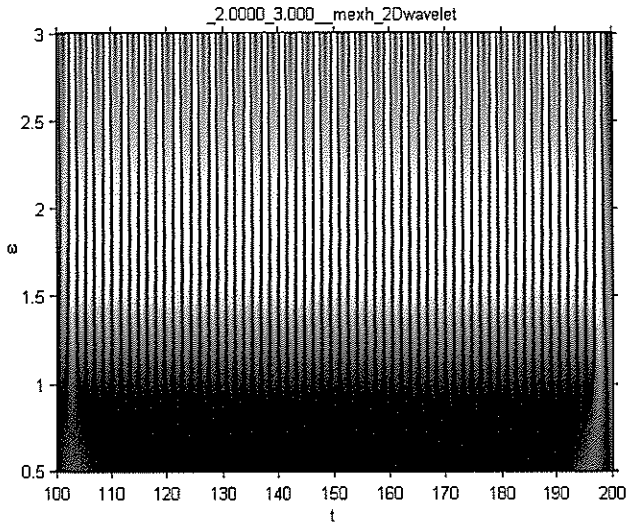

The Gauss-2 wavelet (Mexican hat)

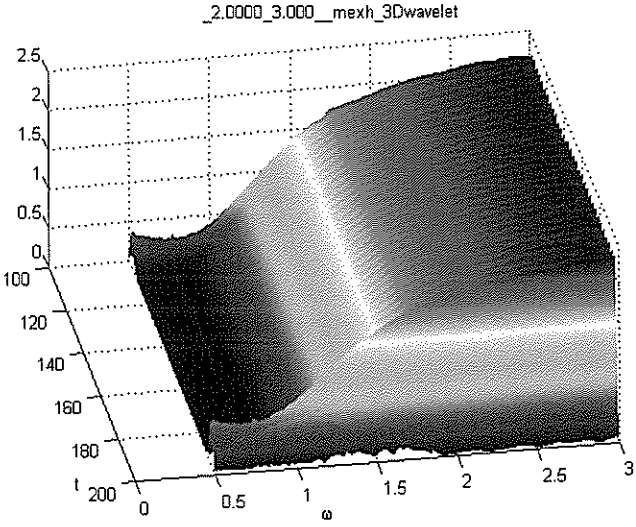

The Gauss-2 wavelet (Mexican hat)

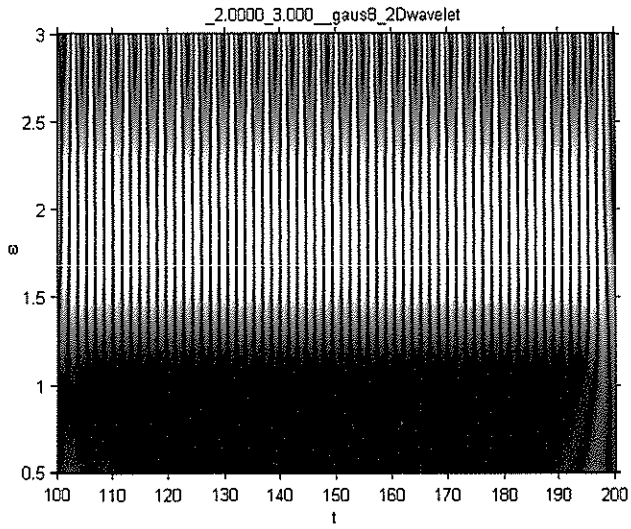

The Gauss-8 wavelet

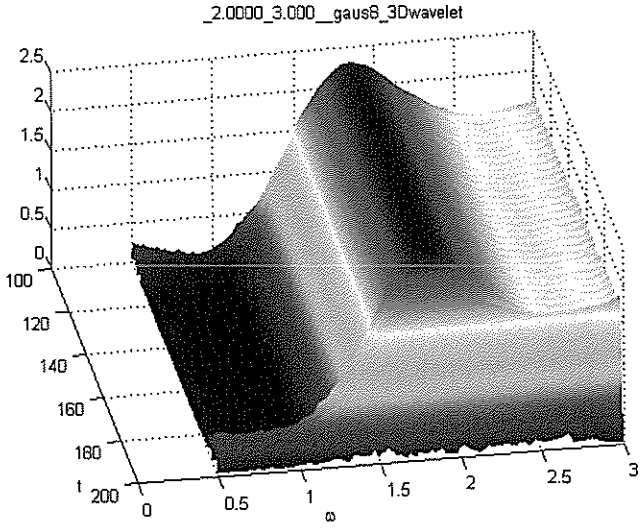

The Gauss-8 wavelet

Table 2. $(\omega = 2; p_x = 7.5)$.

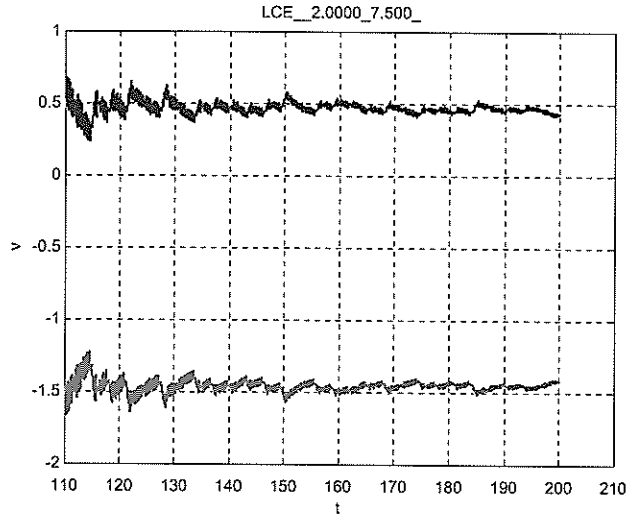

The Lyapunov exponents

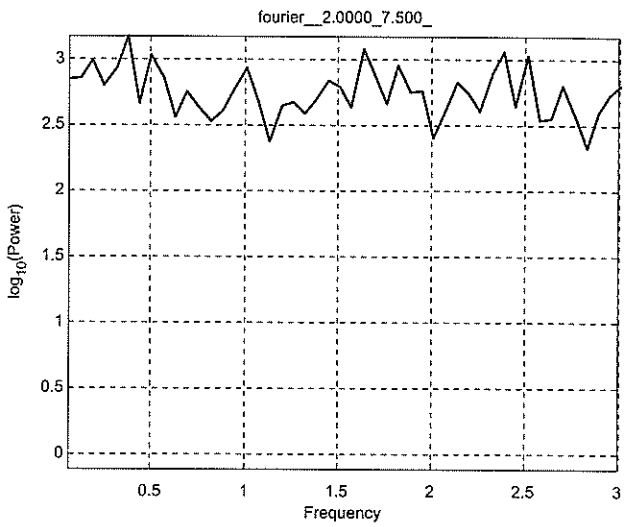

Power spectra

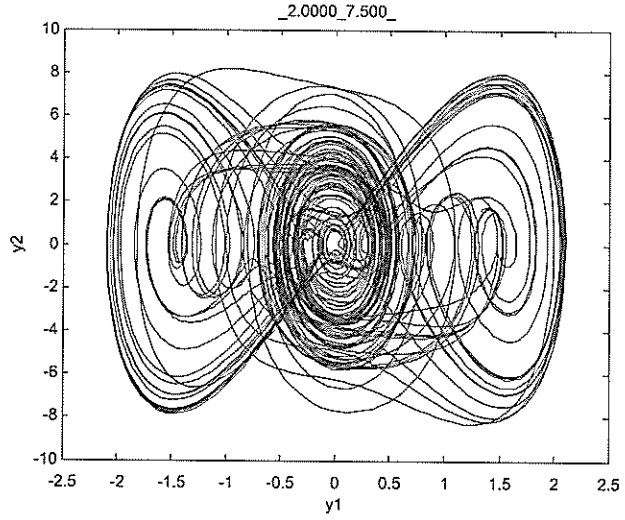

Phase portrait

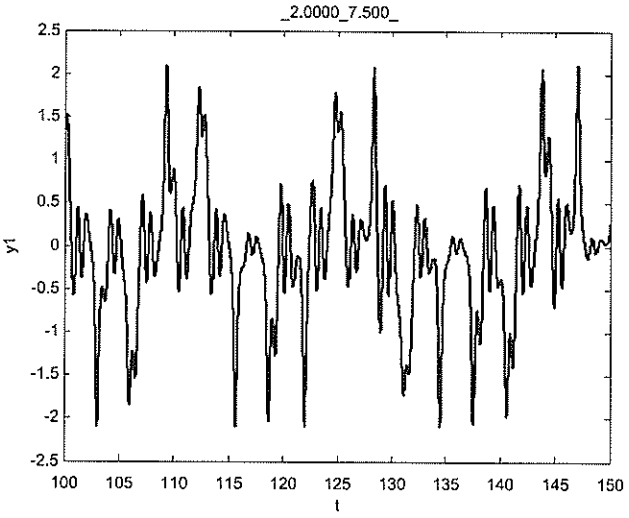

Time history

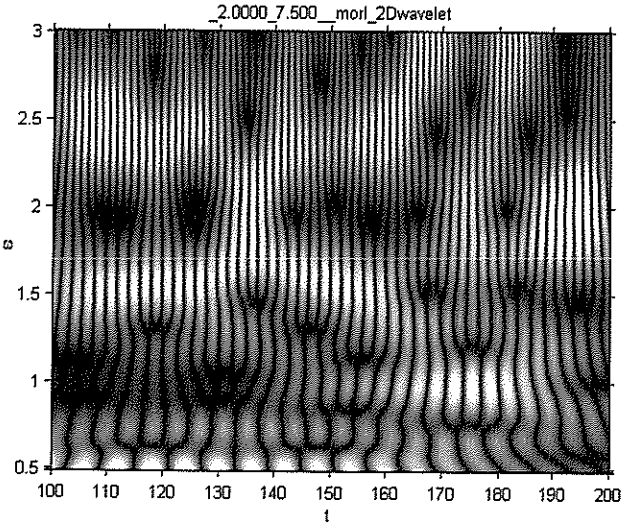

The Morlet wavelet

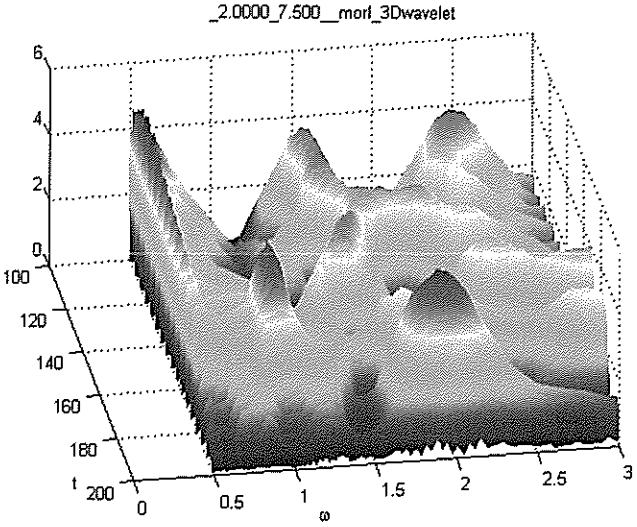

The Morlet wavelet

Table 2. (*Continued*)

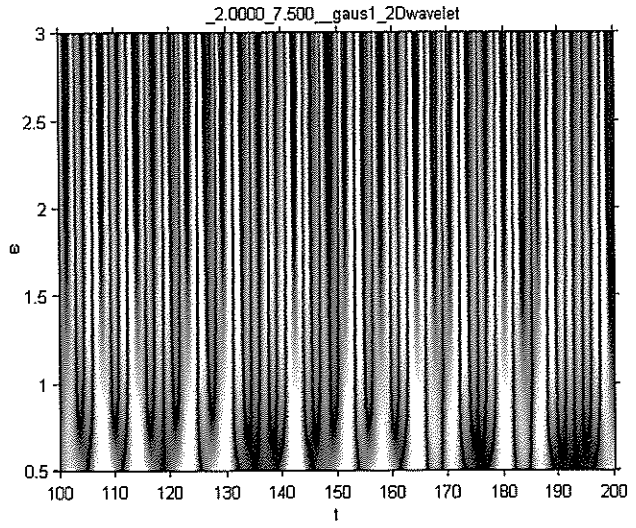

The Gauss-1 wavelet

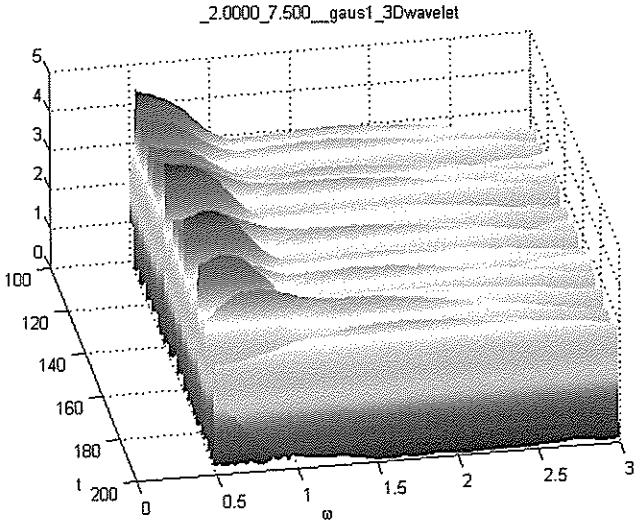

The Gauss-1 wavelet

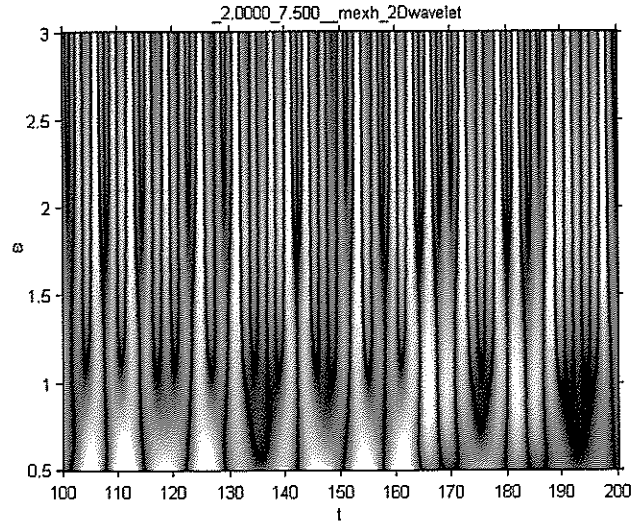

The Gauss-2 wavelet (Mexican hat)

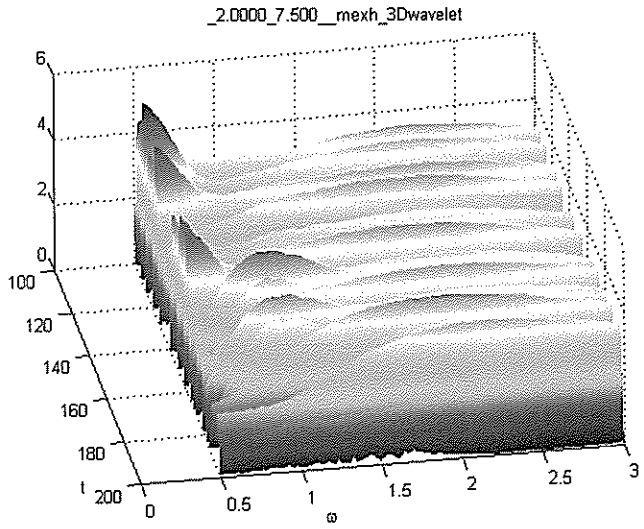

The Gauss-2 wavelet (Mexican hat)

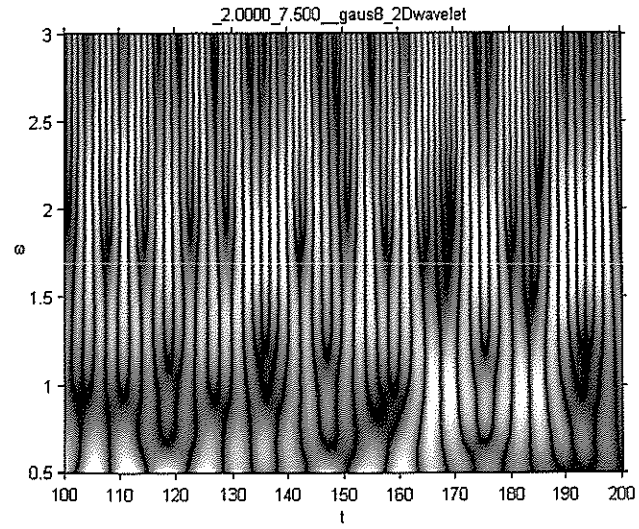

The Gauss-8 wavelet

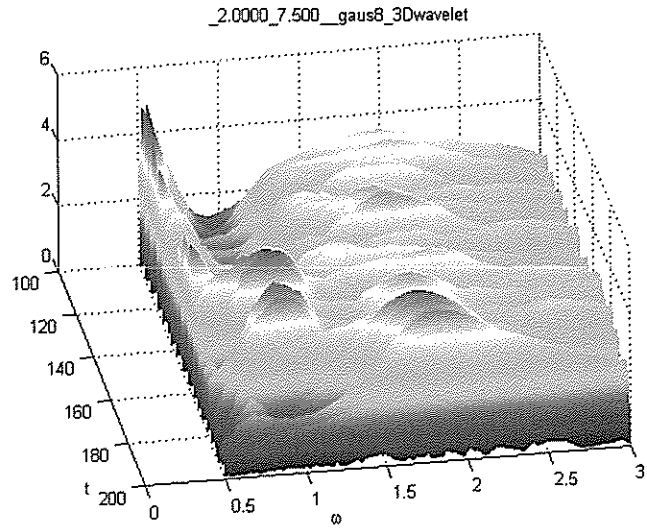

The Gauss-8 wavelet

control parameters (in our case, these are amplitude and frequency of excitation), it may happen that on one time intervals oscillations are regular, whereas on the other they are chaotic ones. In such cases the wavelet-spectrum and the dynamics of the Lyapunov exponents supplement each other giving a reliable picture of the system behavior.

The described situation is given in Table 3. Phase portrait and Fourier spectrum are constructed on the whole time interval, and they clearly testify the occurrence of chaos. However, tracing the Lyapunov exponents evolution, one may observe such time instant, when the largest Lyapunov's exponent changes from positive to negative. It means that the system oscillations are regular. In order to study this time instant we apply wavelet analysis. One may observe the mentioned transition from chaotic to periodic dynamics, but for an earlier time instant than that indicated by the largest Lyapunov exponent. Again it appears that the most suitable, in the sense of frequencies recognition, are the Morlet and the Gauss-8 wavelets.

Knowing time threshold, where transition from chaos to periodicity takes place, one may construct a phase portrait and a Fourier spectrum independently for two time intervals. They are reported in third (up to time instant $t = 150$) and fourth (after $t = 150$) rows of Table 3. They are favorable to the discussed results via wavelet spectra analysis.

Owing to the earlier discussion, it is of interest to introduce the comparison of frequency-temporal wavelet-spectrum and the dynamics of the

Table 3. $(\omega = 2.5; p_x = 7.4)$.

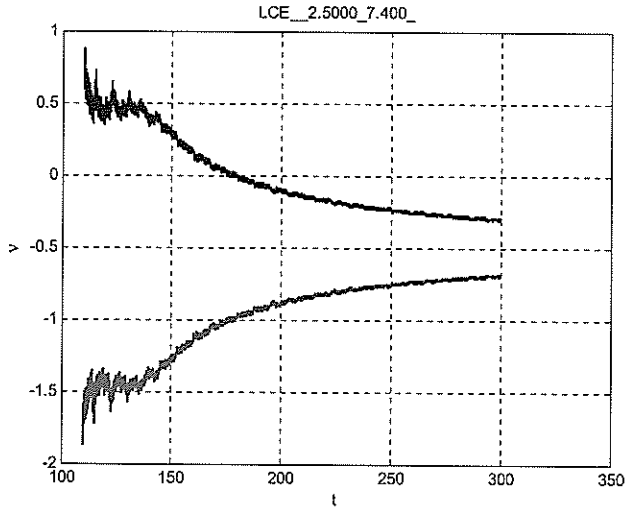

The Lyapunov exponent

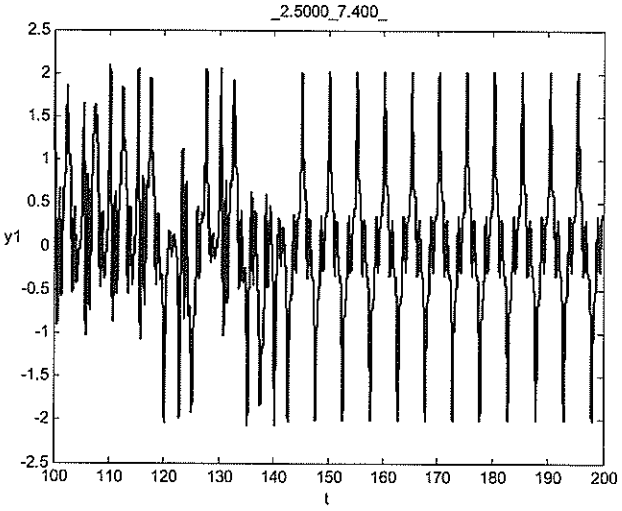

Time history

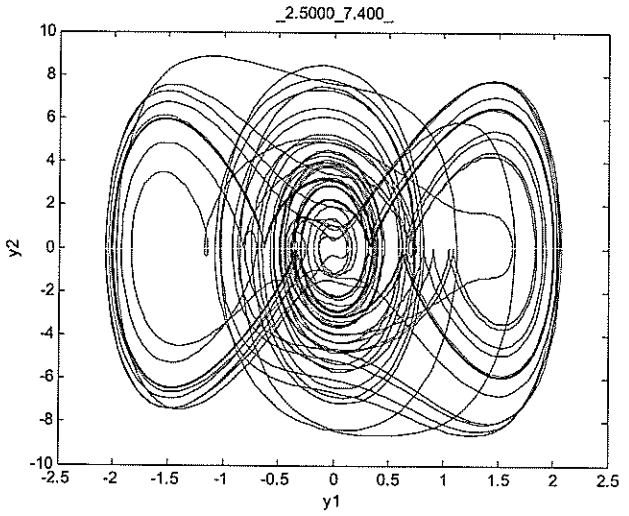

Phase portrait on the whole interval

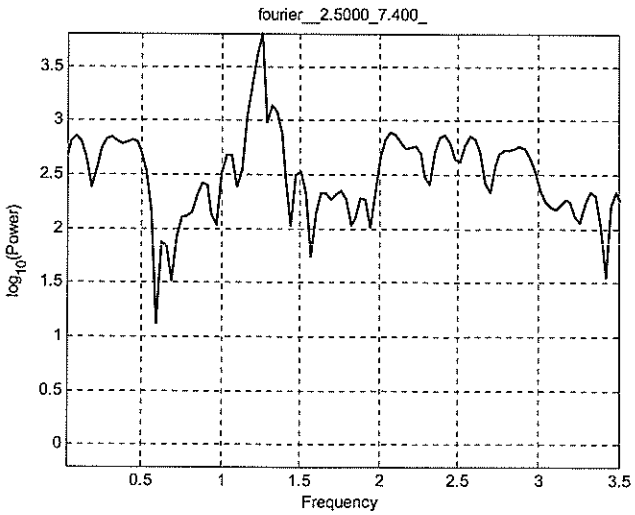

Power spectrum on the whole interval

Table 3. (*Continued*)

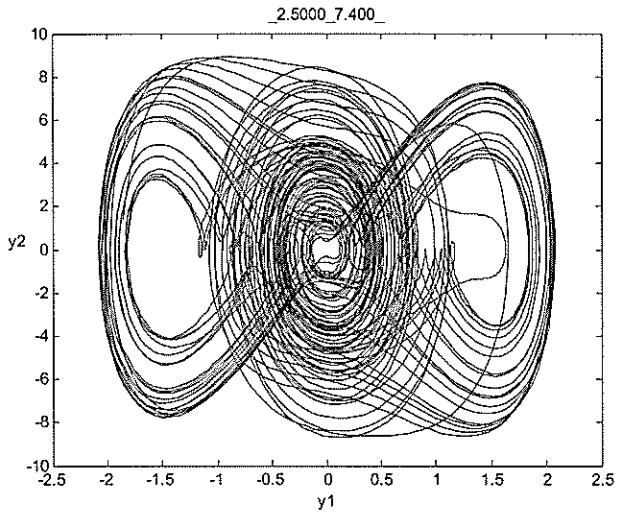

Phase portrait for $t \in [50; 150]$

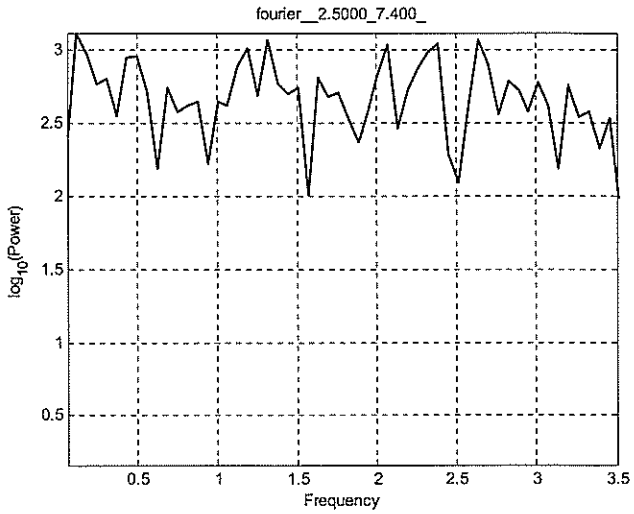

Power spectrum for $t \in [50; 150]$

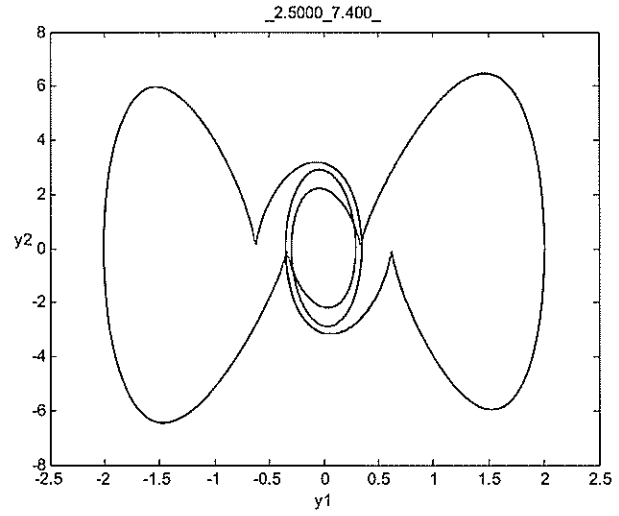

Phase portrait for $t \in [150; 250]$

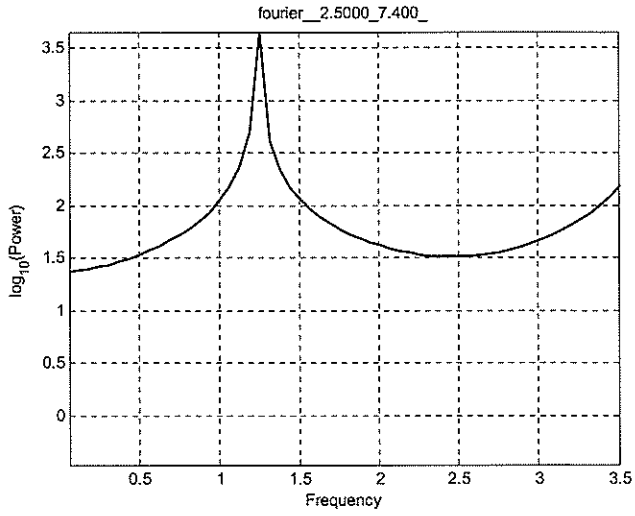

Power spectrum for $t \in [150; 250]$

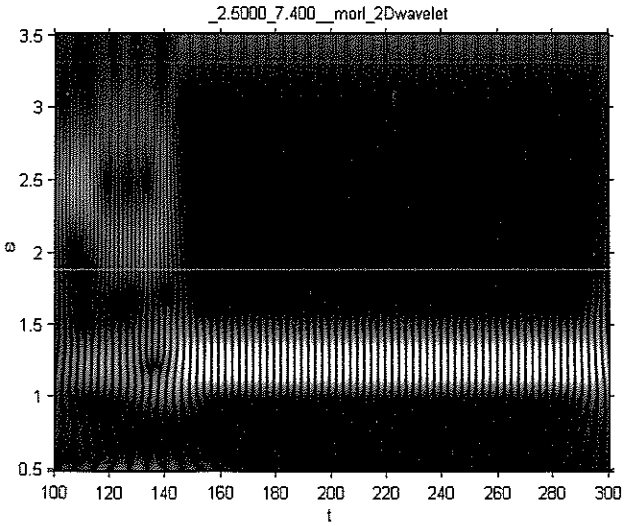

The Morlet wavelet

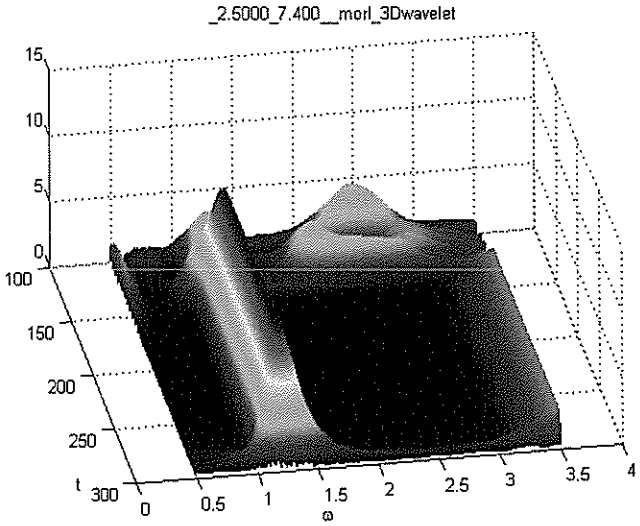

The Morlet wavelet

Table 3. (*Continued*)

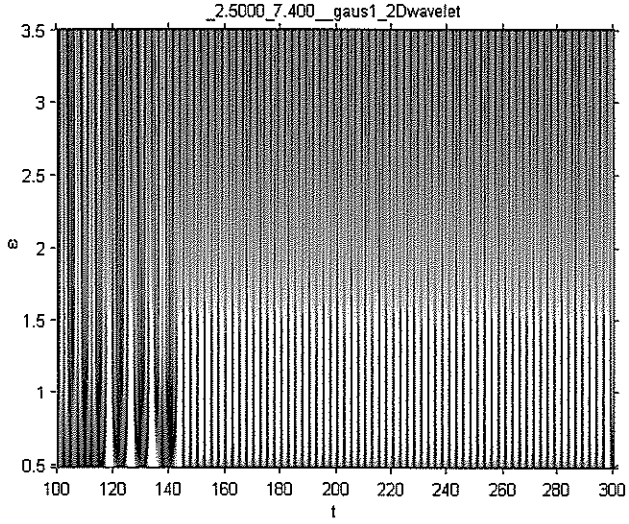

The Gauss-1 wavelet

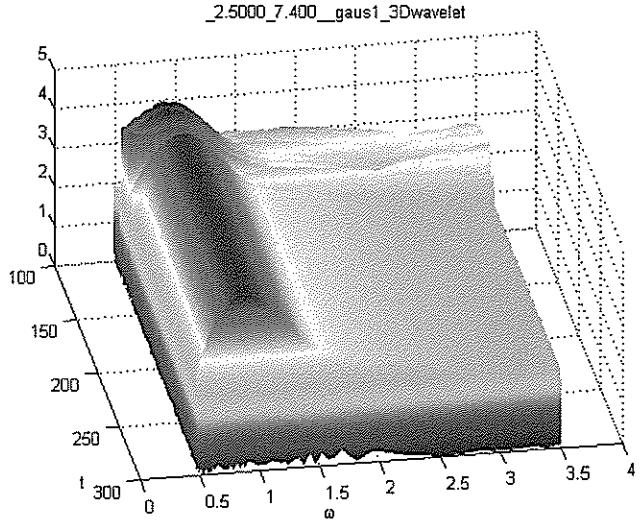

The Gauss-1 wavelet

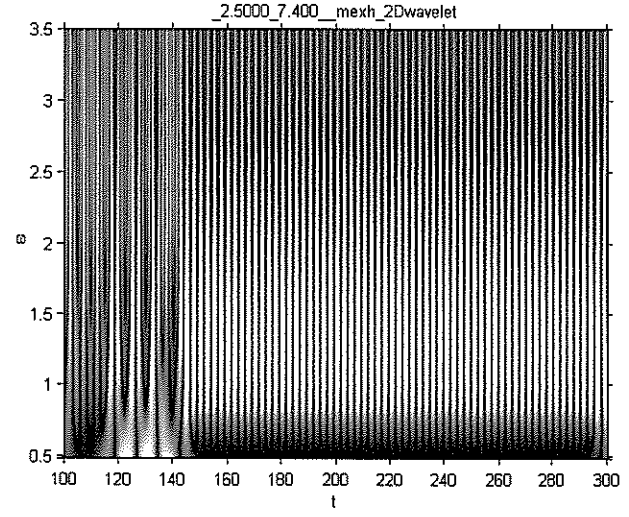

The Gauss-2 wavelet (Mexican hat)

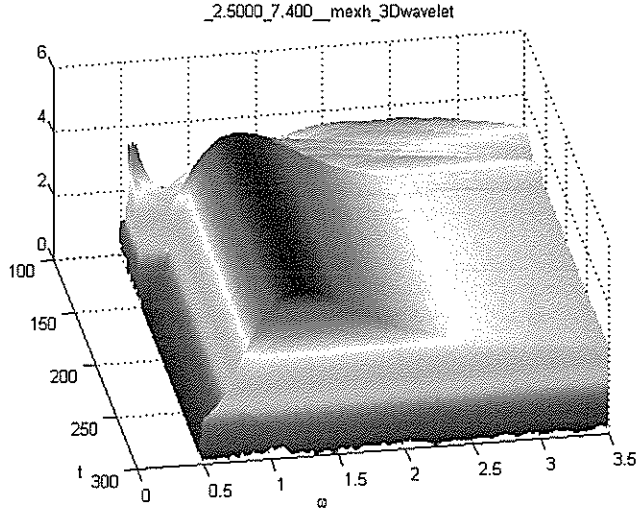

The Gauss-2 wavelet (Mexican hat)

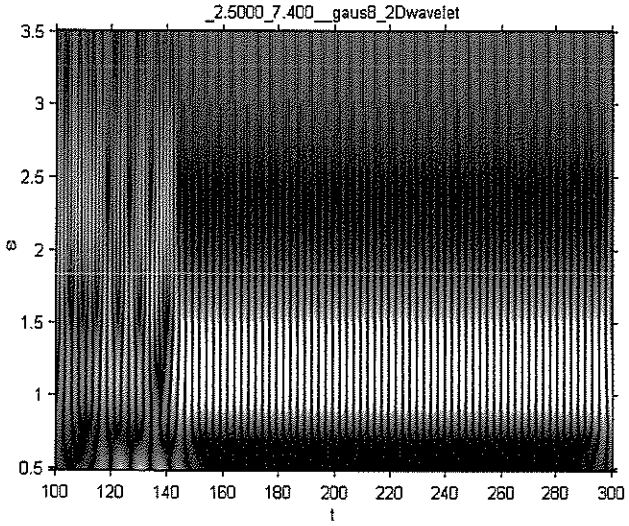

The Gauss-8 wavelet

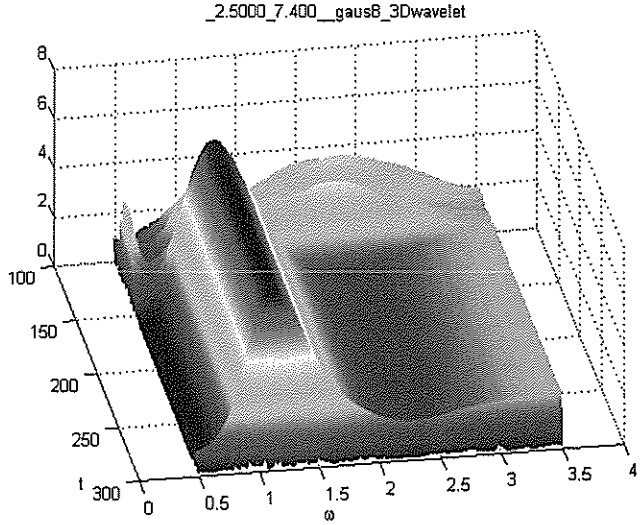

The Gauss-8 wavelet

Table 4. $(\omega = 2.6; p_x = 7.4)$.

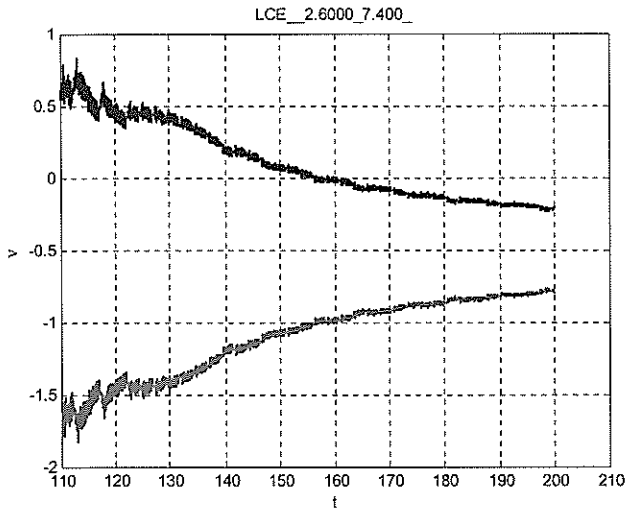

The Lyapunov exponents

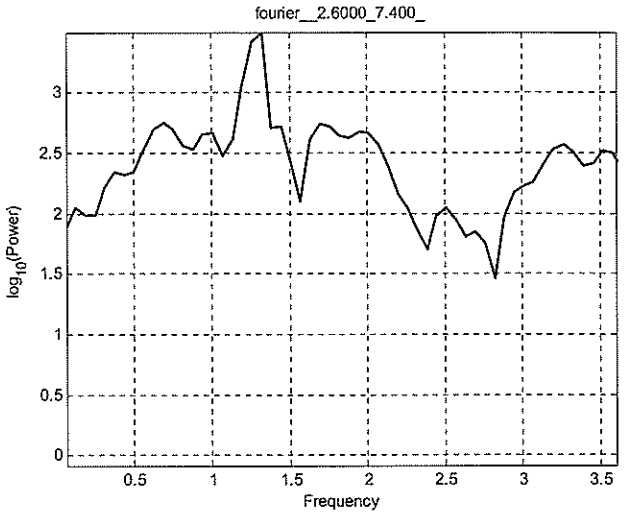

Power spectrum

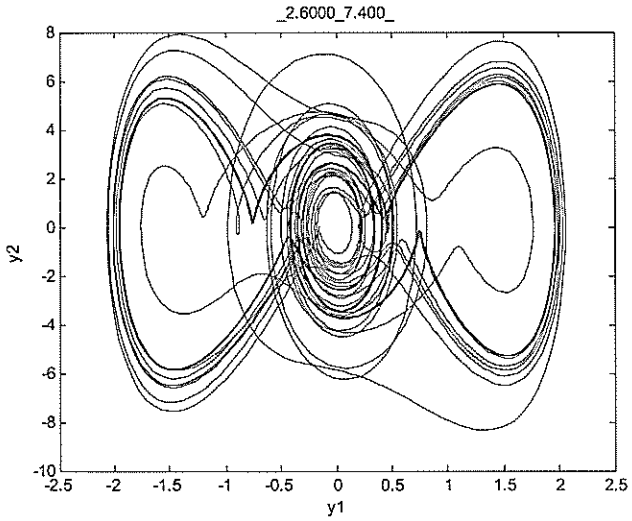

Phase portrait

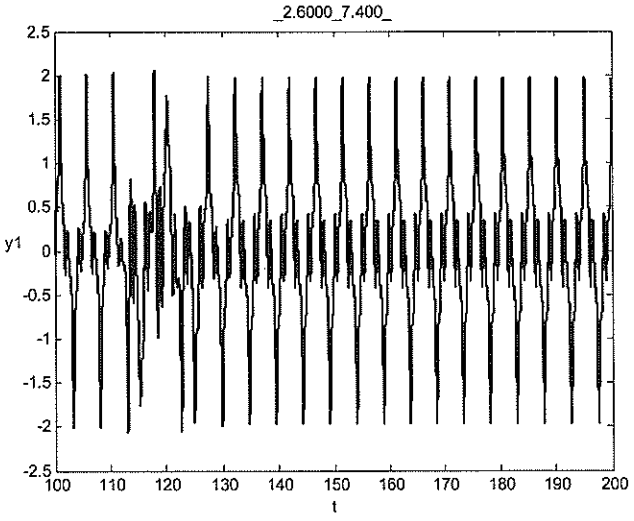

Time history

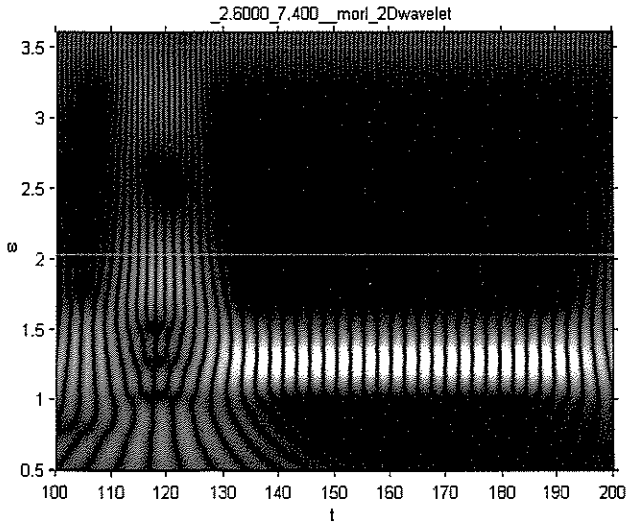

The Morlet wavelet

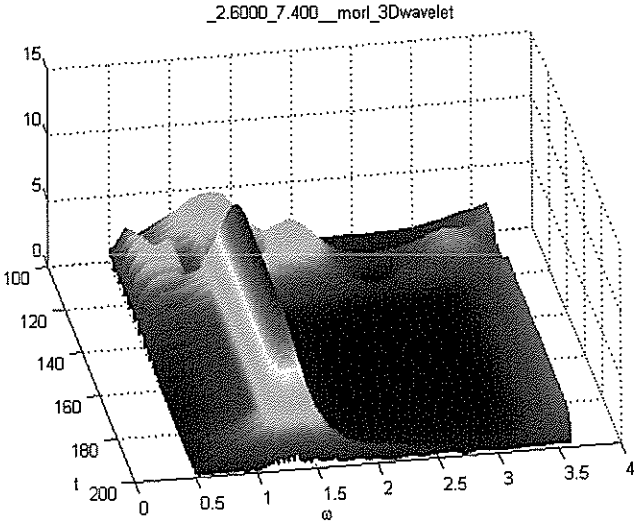

The Morlet wavelet

Table 4. (*Continued*)

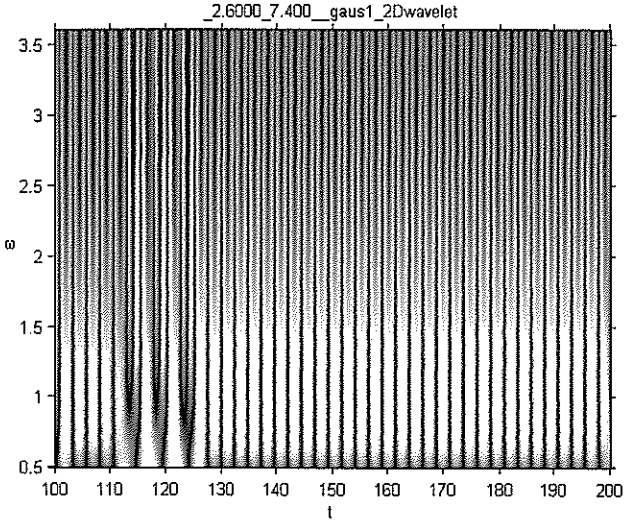

The Gauss-1 wavelet

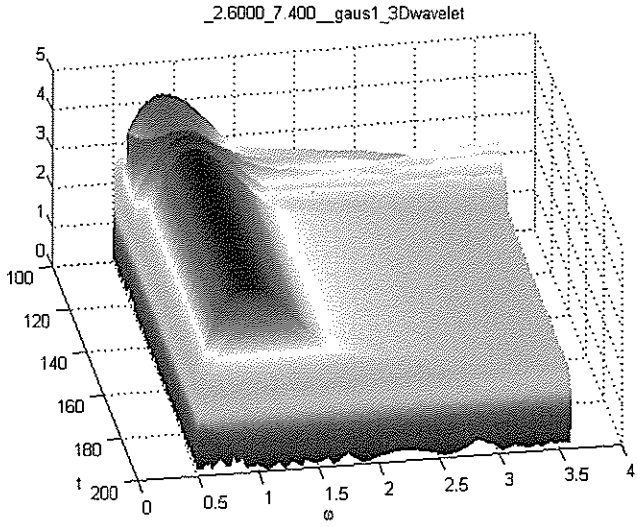

The Gauss-1 wavelet

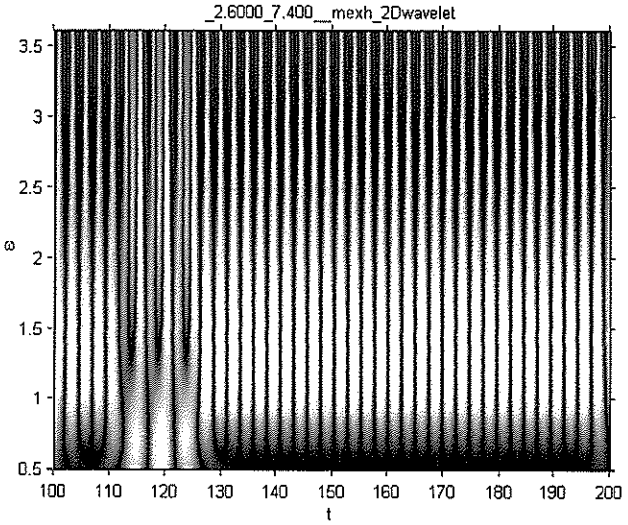

The Gauss-2 wavelet (Mexican hat)

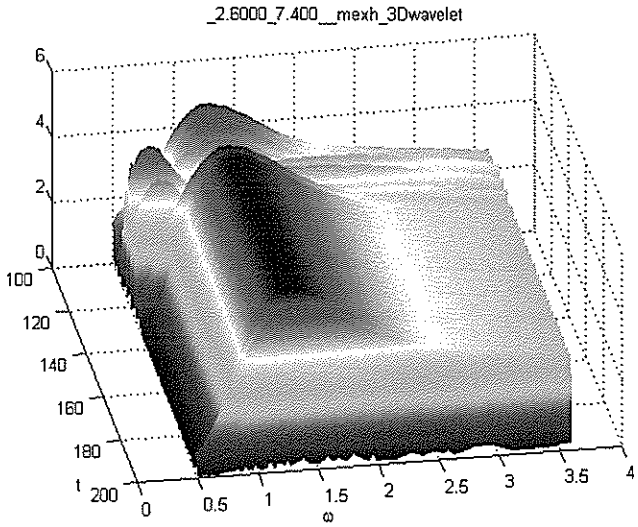

The Gauss-2 wavelet (Mexican hat)

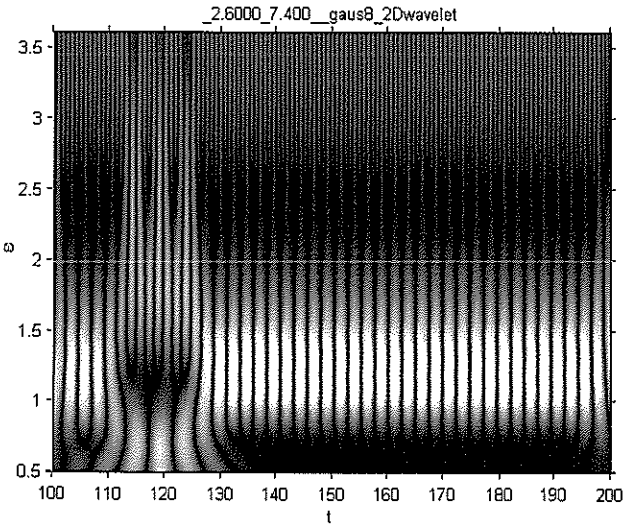

The Gauss-8 wavelet

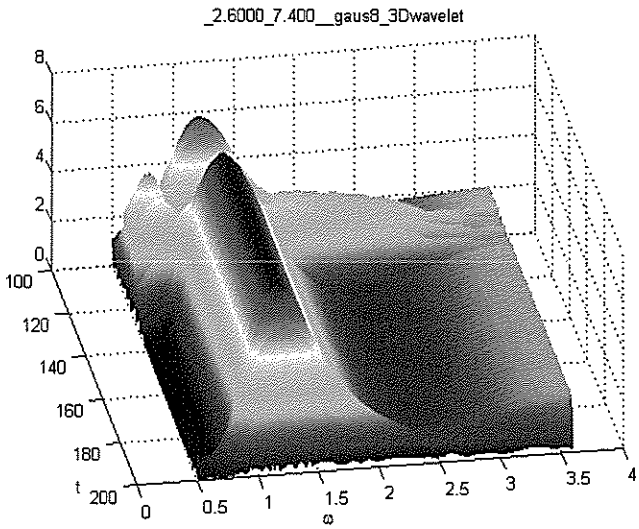

The Gauss-8 wavelet

Table 5. $(\omega = 2.8; p_x = 7.4)$.

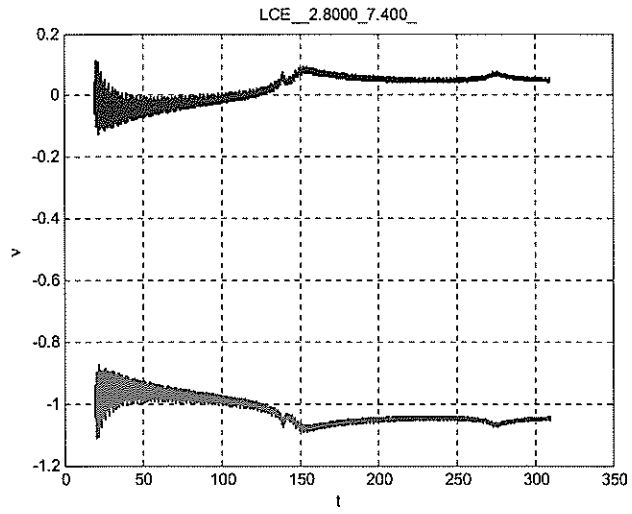

The Lyapunov exponents

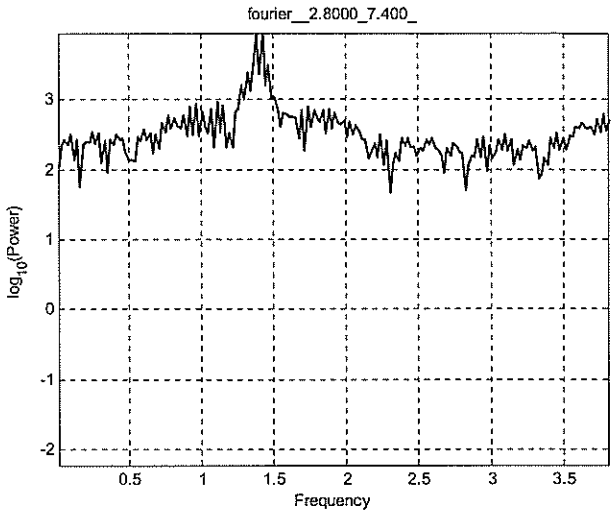

Power spectrum

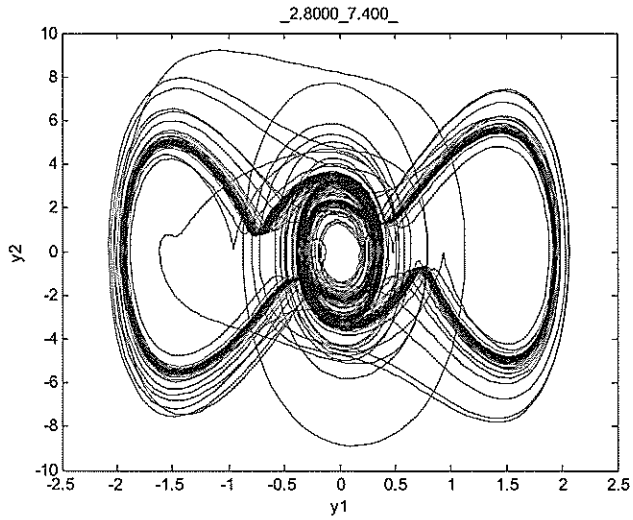

Phase portrait

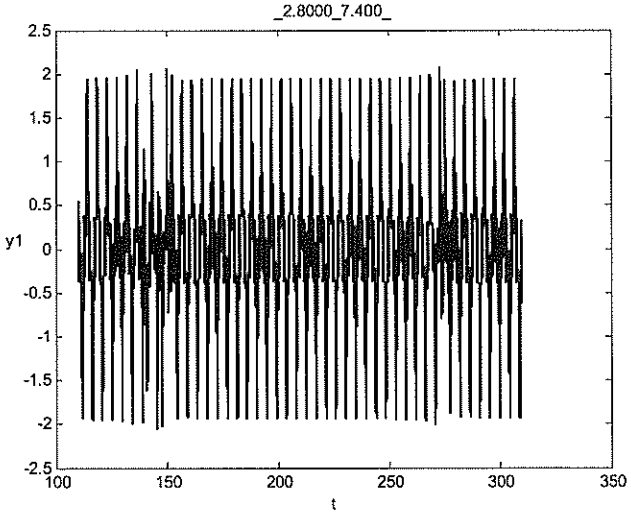

Time history

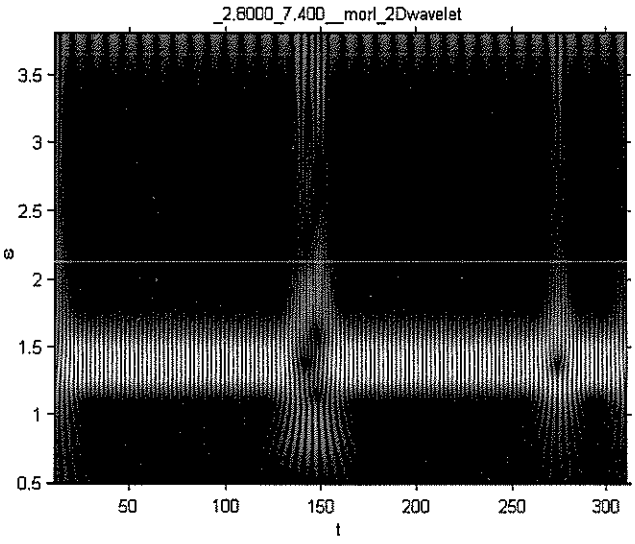

The Morlet wavelet

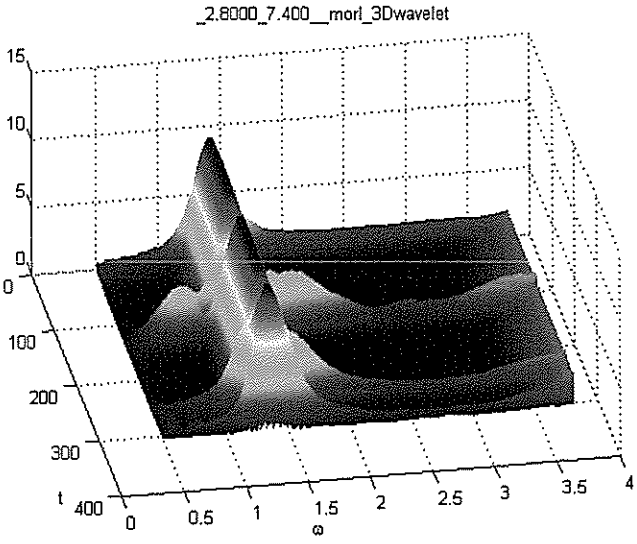

The Morlet wavelet

Table 5. (*Continued*)

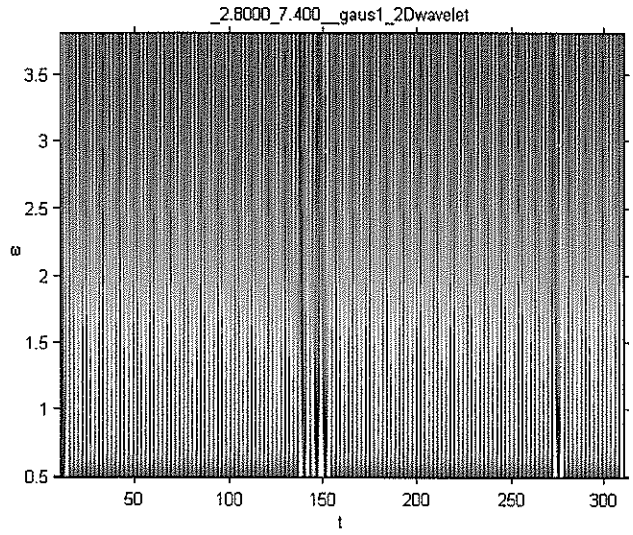

The Gauss-1 wavelet

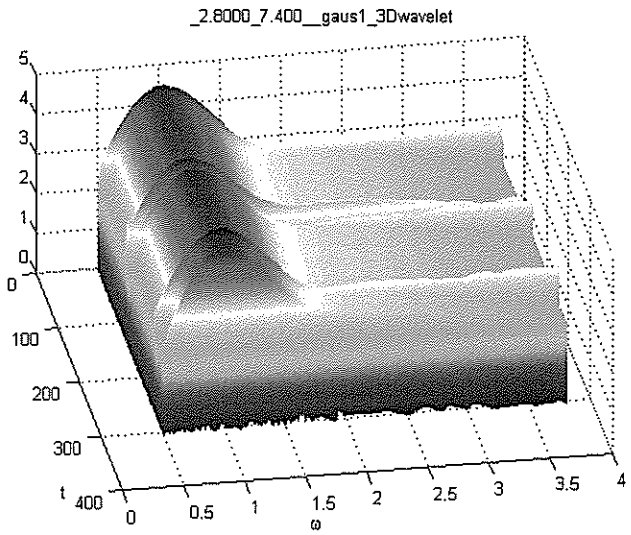

The Gauss-1 wavelet

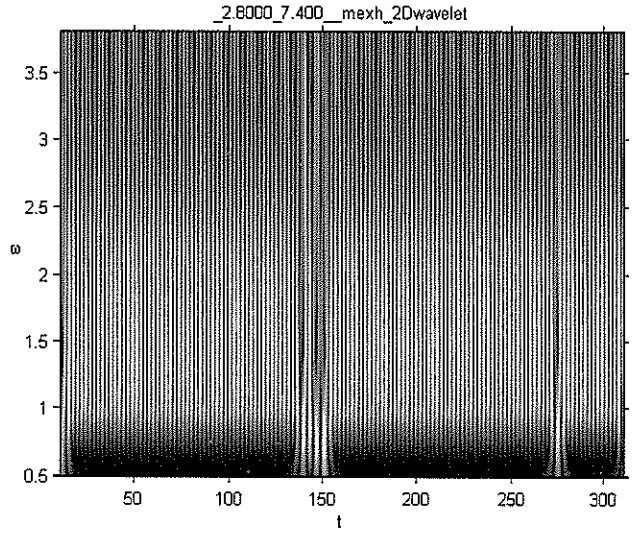

The Gauss-2 wavelet (Mexican hat)

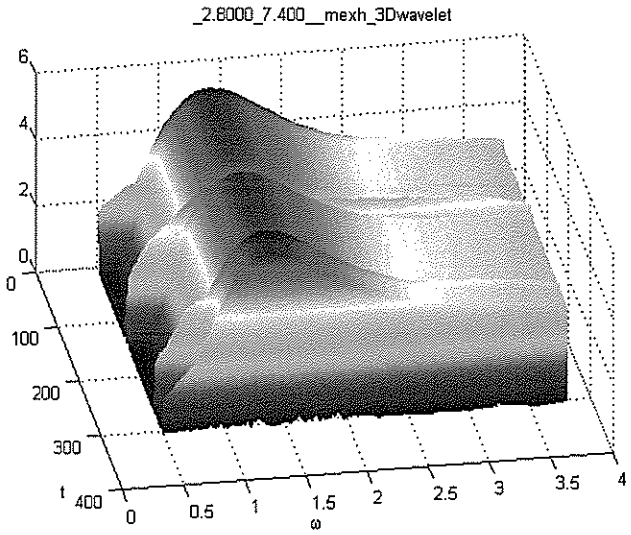

The Gauss-2 wavelet (Mexican hat)

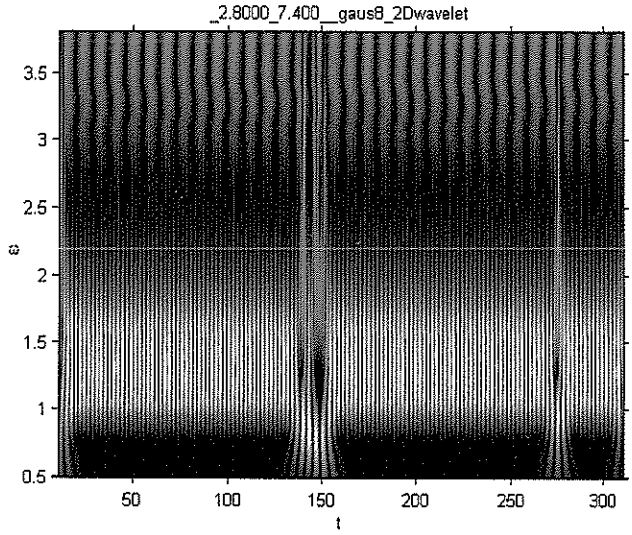

The Gauss-8 wavelet

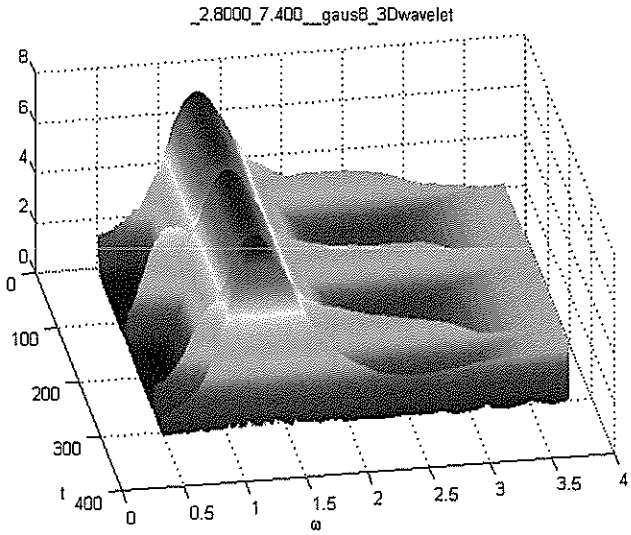

The Gauss-8 wavelet

Lyapunov exponents. Namely, how big is a difference between the estimation of the time instant, where the motion is changed from chaotic to harmonic, while computed via the wavelet analysis and the Lyapunov exponent estimation? Data given in Table 4 suggest that the mentioned difference can be relatively large.

For the control parameters applied in Table 4 a transition from one-frequency vibrations takes place within the time interval of $t \in [130; 140]$ in the case of wavelet based analysis, whereas the Lyapunov exponent becomes negative for $t = 160$. In other words, the Lyapunov exponent is delayed in comparison to the wavelet-transform estimation. However, we have already mentioned that in order to achieve a limit of the Lyapunov exponent time evolution, a rather long computation is required. This is why time interval is expected when the Lyapunov exponent starts to "stabilize" after the change of oscillation character.

Observe that so-far considered cases reported in Tables 1–4 involve rather classical investigations. Namely, relatively long time intervals of either chaotic or regular dynamics have been well represented by the sign of the computed Lyapunov exponents. In Table 5, a less standard case is reported: the wavelet-spectrum exhibits two narrow chaotic windows for time instants $t = 150$ and $t = 275$. Notice that the application of classical tools of analysis like the Fourier spectra and phase portraits fails in this case due to short time intervals. However, the application of the wavelet transforms (in spite of the differences in frequency spectra) allows to overcome the mentioned difficulty, since short time system chaotic regimes are exhibited by all wavelet-spectra.

By neglecting the first transitional Lyapunov exponent dynamics, the following interesting behavior is observed. Already for $t = 100$ the largest Lyapunov exponent being negative becomes positive, and in the time instant corresponding to the first chaotic window, the local maximum of the largest Lyapunov exponent is observed. However, later on the oscillations are regular ones, but the largest Lyapunov exponent is not negative, and also in the time instant associated with second chaotic window occurrence one may observe again its local maximum.

In what follows, we are going to compare the evolution of the largest Lyapunov exponent (curve 2 in Fig. 3) with time history of maximum beam deflection (curve 1 in Fig. 3). It is well known that jump-like change of maximal deflection corresponds to a stiff stability loss. As the results presented in Fig. 3 show, in the time instants associated with stability loss the largest Lyapunov exponent is either positive or exhibits its increase tendency.

In the above, we have illustrated and discussed regular and chaotic beam dynamics and its quantification via the Lyapunov exponent estimation. The reported results concern two control parameters, i.e. longitudinal load amplitude

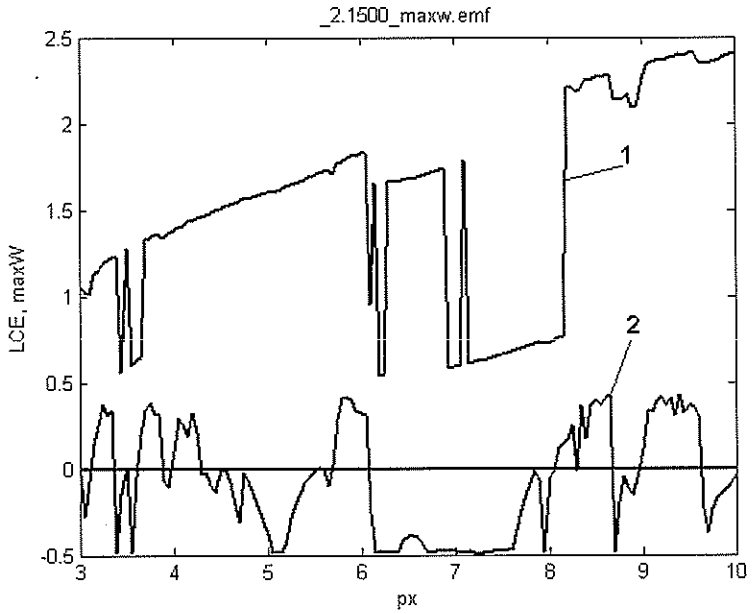

Fig. 3. The Lyapunov exponent (2) and the beam deflection (1), $\omega = 2.15$

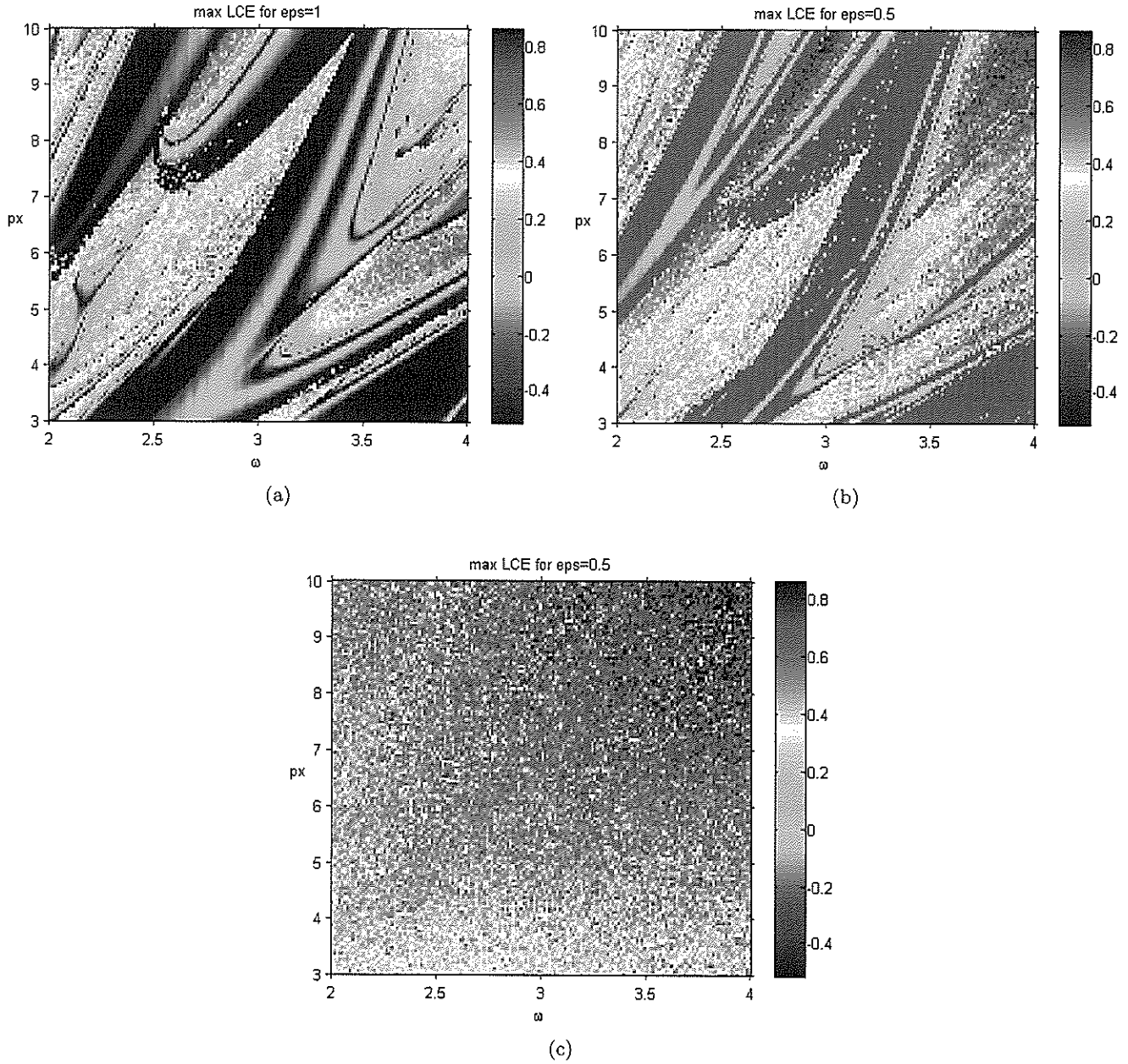

Fig. 4. The largest Lyapunov exponent in the $\{p_x, \omega\}$ plane for various damping coefficients: (a) $\varepsilon = 1$; (b) $\varepsilon = 0.5$ and (c) $\varepsilon = 0$.

and its excitation frequency. In what follows, we compute the largest Lyapunov exponent for each pair of the mentioned control parameters p_x, ω and the so-called "vibration chart" is constructed [see Figs. 4(a)–4(c)].

One may observe how the chart changes with respect to change of damping coefficient ε in the Duffing equation [Figs. 4(a)–4(c)]. It is visible that decreasing damping yield increases the chaotic zones, and finally for $\varepsilon = 0$ the whole chart $\{p_x, \omega\}$ represents chaotic dynamics.

7. The Lyapunov Dimension

It is known that a trajectory of any dynamical system being in chaos is characterized by a chaotic attractor, which can be quantized by its dimension. There exist a few algorithms devoted to dimension computation. In this work, we apply the method of a strange attractor dimension computation proposed by Kaplan and Yorke [1979a, 1979b, 1979c]. Let the dimension of the phase space of the investigated dynamical system be N, so we have N Lyapunov exponents $\lambda_1, \ldots, \lambda_n$. Then the sum $S_m = \sum_{i=1}^{m} \lambda_i$

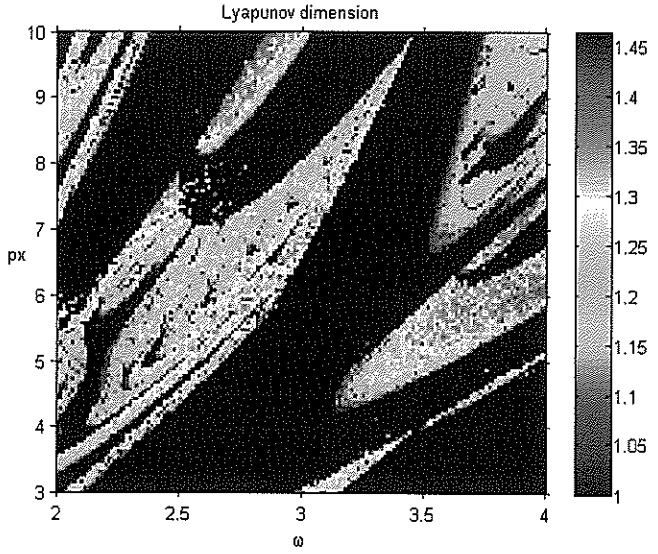

Fig. 5. The Lyapunov dimension chart.

is successively computed. Since the largest Lyapunov exponent of a chaotic attractor is positive, then there exists such m, where $S_m > 0$, and $S_{m+1} < 0$. Owing to Kaplan and Yorke proposal, the after sought dimension is estimated via the following relation:

$$D = m + \frac{\sum_{i=1}^{m} \lambda_i}{|\lambda_{m+1}|}.$$

The latter relation is used for our system dimension chart, shown in Fig. 5, where the same notion as in the previous cases hold.

8. Conclusions

In general, all transitions of the investigated system from its regular to chaotic dynamics and vice versa are detected and illustrated by all testified wavelets. However, the analysis carried out indicates that only two wavelets (the Morlet and the Gauss of eighth order) yield reliable frequency estimation results, and in applications devoted to nonlinear mechanics, the Morlet wavelet transform is mostly recommended. In addition, we have illustrated the links between the largest Lyapunov exponents computation and the wavelet spectra numerical estimation. The reported delay of the largest Lyapunov exponent in comparison to the results yielded by the wavelet transform computation occurs due to the memory property of the investigated system.

References

Al-Raheem, K. F., Roy, A. Ramachandran, K. P., Harison, D. K. & Garinger, S. [2008] "Application of the Laplace wavelet combined with ANN for rolling bearing fault diagnosis," *J. Vibr. Acoust. Trans. ASME* **130**, 051007.

Astafieva, N. W. [1996] "Wavelet analysis: Theoretical background and examples of application," UFN **11**, 1145–1170 (in Russian).

Awrejcewicz, J., Narkaitis, G. G. & Krysko, V. A. [2002] "Bifurcations of a thin plate-strip excited transversally and axially," *Nonlin. Dyn.* **32**, 187–209.

Awrejcewicz, J. & Krys'ko, V. A. [2003a] *Nonclassical Thermoelastic Problems in Nonlinear Dynamics of Shells* (Springer, Berlin).

Awrejcewicz, J. & Krys'ko, V. A. [2003b] "Wavelets-based analysis of parametric vibrations of flexible plates," *Int. J. Appl. Mech.* **39**, 3–43.

Awrejcewicz, J. & Krys'ko, V. A. [2006] *Introduction to Asymptotic Methods* (Chapman & Hall/CRC).

Awrejcewicz, J., Krys'ko, V. A. & Krys'ko, A.V. [2007] *Thermo-Dynamics of Plates and Shells* (Springer, Berlin).

Bayissa, W. L., Haritos, N. & Thelandersson, S. [2008] "Vibration-based structural damage identification using wavelet transform," *Mech. Syst. Sign. Process.* **22**, 1194–1215.

Bennettin, G., Galgani, L. & Strelcyn, I. M. [1976] "Kolmogorov entropy and numerical experiments," *Phys. Rev. A* **14**, 238.

Bennettin, G., Galgani, L., Giorgilli, A. & Strelcyn, I. M. [1980] "Lyapunov characteristic exponents for smooth dynamical systems and for Hamiltonian systems; a method for computing all of them," *Meccanica* **15**, 21–30.

Bennettin, G. & Galgani, L. [1979] *Intrinsic Stochasticity in Plasmas*, eds. Laval, G. (Lies Edition de Physique, Courtraboeut: Orsay), p. 93.

Chui, C. K. Wavelets [1997] *A Mathematical Tool for Signal Analysis* (SIAM, Philadelphia).

Daubechies, I. [1991] *Ten Lectures on Wavelets* (SIAM, Philadelphia).

Daubechies, I. & Sweldens, W. [1998] "Factoring wavelet transforms into lifting steps," *J. Fourier Anal. Appl.* 4, 247–269.

Fedorova, A. N. & Zeitlin, M. G. [1998] "Wavelets in optimization and approximations," *Math. Comput. Simul.* **46**, 527–534.

Ghanem, R. & Romeo, F. A. [2001] "Wavelet-based approach for model and parameter identification of non-linear systems," *Int. J. Non-Lin. Mech.* **36**, 835–859.

Grossman, A. & Morlet, S. [1984] "Decomposition of hardy functions into square separable wavelets of constant shape," *SIAM J. Math. Anal.* **15**, 723.

Guckenheimer, J. & Holmes, P. [1983] "*Nonlinear Oscillations, Dynamical Systems, and Bifurcations of Vector Fields* (Springer, NY).

Holmes, P. [1979] "A nonlinear oscillator with a strange attractor," *Phil. Trans. R. Soc. Lond. A* **292**, 419–448.

Homles, P. & White, D. [1983] "On the attracting set for duffing equation," *Physica D* **7**, 111–123.

Jeong, H. [2001] "Analysis of plane wave propagation in anisotropic laminates using a wavelet transform," *NDT & E Int.* **34**, 185–190.

Ji, Y. F. & Chang, C. C. [2008] "Nontarget stereo vision technique for spatiotemporal response measurement of line-like structures," *J. Engin. Mech.* **134**, 466–474.

Kaplan, J. L. & Yorke, J. A. [1979] "A chaotic behaviour of multi-dimensional differential equations," in *Functional Differential Equations and Approximations of Fixed Points*. Lecture Notes in Mathematics, Vol. 730. eds. Peitgen, H. O. & Walther, H. O. (Springer, Berlin, NY), pp. 204–227.

Kaplan, J. L. & Yorke, J. A. [1979] "Preturbulence: A regime observed in a fluid flow model of Lorenz," *Commun. Math. Phys.* **67**, 93.

Kaplan, J. L. & Yorke, J. A. [1979] "The onset of chaos in a fluid flow model of Lorenz," *Ann. N.Y. Acad. Sci.* **316**, 400.

Konishi, K. [2001] "Making chaotic behaviour in a damped linear harmonic oscillator," *Phys. Lett. A.* **284**, 85–90.

Lepik, Ü. [2001] "Application of wavelet transform techniques to vibration studies," *Proc. Estonian Acad. Sci. Phys. Math.* **50**, 155–168.

Lepik, Ü. [2003] "Exploring irregular vibrations and chaos by the wavelet method," *Proc. Estonian Acad. Sci.* **9**, 3–24.

Lepik, Ü. [2007] " Application of the Haar wavelet transform to solving integral and differential equations," *Proc. Estonian Acad. Sci. Phys. Math.* **56**, 28–46.

Li, F., Meng, G., Ye, L. & Chen, P. [2008] "Wavelet transform-based higher-order statistics for fault diagnosis in rolling element bearings," *J. Vibr. Contr.* **14**, 1691–1709.

Liu, B. [2003] "Adaptive harmonic wavelet transform with applications in vibration analysis," *J. Sound Vibr.* **262**, 45–64.

Loutridis, S., Douke, E., Hadjileontiadis, L. J. & Trochidis, A. [2005] "A two-dimensional wavelet transrom for detection of cracks in plates," *Engin. Struct.* **27**, 1327–1338.

Messina, A. [2008] "Refinements of damage detection methods based on wavelet analysis of dynamical shapes," *Int. J. Solids Struct.* **45**, 4068–4097.

Moslehy, F. A. & Evan-Iwanowski, R. M. [1991] "The effects of non-stationary processes on chaotic and regular responses of the Duffing oscillator," *Int. J. Non-Lin. Mech.* **26**, 61–71.

Nayfeh, A. H. & Mook, D. T. [1979] *Nonlinear Oscillation.*

Nayfeh, A. H. & Balachandran, B. [1995] *Applied Nonlinear Dynamics* (John Wiley, NY).

Newland, D. E. [1993] *Introduction to Random Vibrations, Spectral and Wavelet Analysis* (Longman, NY).

Nouira, H., Foltete, E., Alt Brik, B., Hirsinger, L. & Ballandras, S. [2008] "Experimental characterization and modeling of microsliding on a small cantilever quartz beam," *J. Sound Vibr.* **317**, 30–49.

Oseledec, V. I. [1968] *Works of Moscow Mathematical Society* **19**, 179.

Patsias, S. & Staszewski, W. J. [2002] "Damage detection using optical measurements and wavelets," *Structr. Health Monitoring* **1**, 5–22.

Permann, D. & Hamilton, I. [1992] "Wavelet analysis of time series for the Duffing oscillator: The detection of order within chaos," *Phys. Rev. Lett.* **69**, 2607–2610.

Ribeiro, P. [2001] "The second harmonic and the validity of Duffing equation for vibration of beams with large displacements," *Comput. Struct.* **79**, 107–117.

Sanz, J., Perera, R. & Huerta, C. [2007] "Fault diagnosis of rotating machniery based on auto-associate neural networks and wavelet transforms," *J. Sound Vibr.* **302**, 981–999.

Staszewski, W. J. [1998] "Identification of non-linear systems using multi-scale ridges and skeletons of the wavelet transform," *J. Sound Vibr.* **214**, 639–665.

Staszewski, W. J. & Robertson, A. N. [2007] "Time-frequency and time-scale analyses for structural health monitoring," *Philos. Trans. Roy. Soc. A: Mathematical, Physical and Engineering Sciences* **365**, 449–477.

Volmir, A. S. [1972] *Nonlinear Dynamics Plates and Shells* (Moscow, Science).

Wong, L. A. & Chen, J. C. [2001] "Nonlinear and chaotic behaviour of structural system investigated by wavelet transform techniques," *Int. J. Non-Lin. Mech.* **36**, 221–235.

Xiaoping, Y. [2001] "Lagrange stability for asymmetric Duffing equations," *Nonlin. Anal.* **43**, 137–151.

Yang, J. M., Hwang, C. N. & Yang, B. L. [2008] "Crack identification in beams and plates by discrete wavelet transform method," *J. Ship Mech.* **12**, 464–472.

Zheng, J., Gao, H. & Guo, Y. [1998] "Application of wavelet transform to bifurcations and chaos study," *Appl. Math. Mech.* **19**, 593–599.

Zhong, G.-S., Fang, Y.-G. & Xu, G.-Y. [2008] "Study on blasting vibration effect assessment of structure based on wavelet transform," *J. Vibr. Shock* **27**, 121–124, 129.

Zhong, S. & Oyadiji, S. O. [2008] "Identification of cracks in beams with auxiliary mass spatial probing by stationary wavelet transform," *J. Vibr. Acoust. Trans. ASME* **130**, 041001.

Zhu, B., Leung, A. Y. T., Wong, C. K. & Lu, W. Z. [2008] "On-line health monitoring and damage detection of structures based on the wavelet transform," *Int. J. Struct. Stab. Dyn.* **8**, 367–387.